Insurance Mathematics and Economics 118 (2024) 72–94

Contents lists available at ScienceDirect

Insurance: Mathematics and Economics

journal homepage: www.elsevier.com/locate/ime

# Benefit volatility-targeting strategies in lifetime pension pools ☆

Jean-François Bégin *, Barbara Sanders

*Department of Statistics and Actuarial Science, Simon Fraser University, 8888 University Drive, Burnaby, British Columbia, V5A 1S6, Canada*

ARTICLE INFO

*JEL classification:*
G22
G11
J11

*Keywords:*
Pooled annuity
Investment risk
Longevity risk
Investment-linked annuity benefits
Mortality credits

ABSTRACT

Lifetime pension pools—also known as group self-annuitization plans, pooled annuity funds, and retirement tontines in the literature—allow retirees to convert a lump sum into lifelong income, with payouts linked to investment performance and the collective mortality experience of the pool. Existing literature on these pools has predominantly examined basic investment strategies like constant allocations and investments solely in risk-free assets. Recent studies, however, proposed volatility targeting, aiming to enhance risk-adjusted returns and minimize downside risk. Yet they only considered investment risk in the volatility target, neglecting the impact of mortality risk on the strategy. This study thus aims to address this gap by investigating volatility-targeting strategies for both investment and mortality risks, offering a solution that keeps the risk associated with benefit variation as constant as possible through time. Specifically, we derive a new asset allocation strategy that targets both investment and mortality risks, and we provide insights about it. Practical investigations of the strategy demonstrate the effectiveness and robustness of the new dynamic volatility-targeting approach, ultimately leading to enhanced lifetime pension benefits.

## 1. Introduction

As the prevalence of guaranteed pension arrangements decreases worldwide, there is a growing expectation that flexible retirement schemes like lifetime pension pools will gain popularity. Lifetime pension pools allow retiring individuals to convert a lump sum into income for life. Unlike traditional pension plans, these pools do not provide a fixed or guaranteed level of income. Instead, the pension payouts are contingent upon the performance of the underlying investments and the collective mortality experience of the pool members.

Various arrangements, products, and monikers fit the broad description of lifetime pension pools in the literature: group self-annuitization (GSA) plans (Piggott et al., 2005; Valdez et al., 2006; Qiao and Sherris, 2013; Hanewald et al., 2013), pooled annuity funds (Stamos, 2008; Donnelly et al., 2013), annuity overlay funds (Donnelly et al., 2014; Donnelly, 2015), retirement tontines (Milevsky and Salisbury, 2015, 2016; Chen and Rach, 2019; Fullmer, 2019; Iwry et al., 2020; Gemmo et al., 2020; Weinert and Gründl, 2021; Chen et al., 2021), variable annuities (Balter and Werker, 2020; Balter et al., 2020; Dees et al., 2021), and variable payout annuities (Horneff et al., 2010; Boyle et al., 2015). Note that all these designs can be viewed as implicit or explicit tontines.[1]

The design of these pools has primarily been examined within the context of elementary investment strategies, like constant, static allocations and investment strategies that only involve risk-free assets. Yet other cutting-edge strategies might improve the risk–reward profile of the pool

☆ The authors would like to thank the editors and two anonymous referees for their valuable suggestions and comments on the research project. Bégin wishes to acknowledge the financial support of Natural Sciences and Engineering Research Council of Canada (Grant No. RGPIN-2018-04337) and the Canadian Institute of Actuaries (Grant No. AC-ARG-23-01). Bégin and Sanders also acknowledge the financial support of Simon Fraser University. This research was enabled in part by support provided by the Digital Research Alliance of Canada (www.alliancecan.ca).

* Corresponding author.
*E-mail addresses:* jbegin@sfu.ca (J.-F. Bégin), bsanders@sfu.ca (B. Sanders).

[1] Implicit tontines promise to pay the participants an income for life, but longevity credits are not explicitly allocated to the participants; explicit tontines explicitly allocate longevity credits to the individual accounts of participants (see Bernhardt and Donnelly, 2019, for more details).

https://doi.org/10.1016/j.insmatheco.2024.05.006
Received 21 December 2023; Received in revised form 23 May 2024; Accepted 24 May 2024
Available online 6 June 2024

assets and, in turn, yield better benefits for members. Recently, Olivieri et al. (2022) and Li et al. (2022) proposed a volatility-targeting approach for lifetime pension pools.[2] Broadly speaking, the main aim of volatility targeting is to manage a portfolio's risk exposure in such a way that its volatility is as close to the target as possible. It is argued that this strategy can improve the portfolio returns—increase the average and reduce the likelihood of downside risk—because of the well-documented negative relationship between returns and volatility (i.e., Black's *leverage effect*). Put simply, as volatility increases, returns are expected to be negative, thus justifying a smaller allocation to the risky asset. When volatility decreases, on the other hand, returns are expected to be positive, meaning that it is beneficial to invest more aggressively in the risky asset.

Olivieri et al. (2022) and Li et al. (2022) provide guidance on adjusting the asset allocation strategy to target some volatility levels in the context of lifetime pension pools, improving the investment performance while reducing volatility and downside risk. The conclusions of the two articles are similar as they both find that it is beneficial to target volatility. Their methodology, however, only considers investment risk in the volatility target, exposing the pool to uncontrolled mortality risk that can become quite large as pool members get older.[3] As these lifetime pension pools become more popular, understanding how to simultaneously cope with both investment and mortality risks is of paramount importance for the sustainability of these arrangements, especially because members bear all the risks.

In this research, we investigate volatility targeting of the total benefit adjustment—including both investment and mortality risk—so that the risk associated with benefit variation is kept as constant as possible through time. This article offers two contributions to the existing body of literature: one of a theoretical nature and the other applied. On the one hand, we derive an asset allocation strategy that considers both investment and mortality risks at the same time. This derivation is based on simple assumptions used to proxy the benefit volatility, consistent with the idea that the actual data generating process is unknown to the pool operator and she needs to use approximations to identify the volatility. Specifically, we assume that the number of survivors in the pool is given by a binomial distribution with a survival probability based on past information and that future volatility is obtained via a *nonparametric* heterogeneous autoregressive (HAR) model based on high-frequency returns.[4] The HAR model is selected because it is simple to use and produces reliable volatility forecasts.

On the other hand, we investigate the implementation of the volatility-targeting strategy. This assessment relies on a state-of-the-art data generating process—different than the model used by the pool operator to determine the asset allocation. The risk-free rate of return relies on a three-factor Vasicek (1977) model in the spirit of Babbs and Nowman (1999). Risky asset returns are modelled via an affine continuous-time two-factor stochastic volatility model that extends the double Heston model of Christoffersen et al. (2009) by allowing for jumps. This model captures many of the well-known stylized facts in finance. Systematic longevity risk is captured by a Plat (2009) variant of the well-known Cairns et al. (2006) model which allows for the addition of a nonparametric baseline age effect as well as random future improvements modelled via two period effects. This age–period–cohort (APC) model is able to capture past and future variations in life expectancies. Idiosyncratic mortality risk is also accounted for.

Based on random investment and mortality scenarios, we find that the new dynamic volatility-targeting strategy performs well and provides a steady stream of benefits. The volatility-targeting strategy substantially reduces benefit risk by cutting the risky asset allocation when the benefit volatility—either stemming from the risky asset volatility or mortality-induced risk—is high. Multiple tests show that the results are robust to the inclusion of death benefits, smaller pool sizes, and different exogenous volatility targets. We also consider some practical limitations that might hinder the applicability of the volatility-targeting strategy presented in the study. Specifically, we investigate the impact of leverage constraints, brokerage fees, and rebalancing frequencies. The bulk of our results is robust to these changes in our assumptions.

The remainder of the article is organized as follows. Section 2 presents the assumed data generating process used to model financial asset returns and mortality scenarios. The design of the stylized lifetime pension pool under consideration is explained in Section 3. Section 4 describes the process used by the pool operator to target benefit volatility. The implementation of the strategy is assessed in Section 5. Section 6 investigates practical limitations of the volatility-targeting strategy. Section 7 concludes, while proofs of the various propositions and additional results are provided in the supplementary material.

## 2. The assumed data generating process

This study relies on two different sets of models: a first set of models that allows us to generate future realizations of the real world—the assumed data generating process—and a second set that is used by the pool operator to target volatility. It is important to stress at this stage that we do not assume the operator would know the true generating process, and having two sets of models capture this important dimension in our problem. Indeed, understanding the world requires more complicated equations and models while end-users commonly rely on simpler, ad hoc representations of the reality.

This section covers the first set of assumed data generating processes, whereas Section 4 provides details on the second set.

[2] The literature on volatility targeting goes back more than two decades and is overwhelmingly positive (see, e.g., Fleming et al., 2001; Hallerbach, 2012; Hocquard et al., 2013; Moreira and Muir, 2017; Doan et al., 2018; Harvey et al., 2018). The latter studies have demonstrated enhanced Sharpe ratios, reduced maximum drawdowns, and a more consistent risk profile across a diverse range of risk assets and over different time periods. Some recent papers by Liu et al. (2019), Bongaerts et al. (2020), and Mylnikov (2021), however, identified biases in some of these studies—the use of future information in defining the strategy benchmark and the use of risk-adjusted return measures to gauge the profitability of the strategy, among others. Note that our implementation of the strategy does not suffer from these two biases as we do not rely on future information, and we do not use risk-adjusted return measures.

[3] Both articles also considered ad hoc methods to reduce the allocation for older members, without providing a solution that is consistent with the actual mortality risk profile of the pool.

[4] Being able to accurately forecast volatility is of paramount importance for volatility targeting. Over the years, many parametric models were proposed to forecast volatility in the literature, like the autoregressive conditional heteroscedasticity (ARCH) model of Engle (1982), the generalized ARCH model of Bollerslev (1986), and exponentially weighted moving average-based models. These models were used by Mylnikov (2021) and Olivieri et al. (2022) in the context of volatility targeting, among others. Some other approaches—so-called nonparametric models—rely on realized volatility (i.e., sum of squared intraday high-frequency returns taken over a day). These powerful approaches, pioneered by Corsi (2009), use HAR models to forecast volatility (see Andersen et al., 2007; Busch et al., 2011; Corsi and Renò, 2012; Audrino and Knaus, 2016, for other contributions on the topic). In the context of volatility targeting, Li et al. (2022) used realized volatility to forecast volatility.

### 2.1. A model for financial asset returns

Financial asset returns and prices are important puzzle pieces to grasp investment risk in lifetime pension pools. For simplicity's sake, we assume that the pool can invest in two assets: a risk-free asset and a risky asset. The risk-free rate of return is modelled using a three-factor Vasicek (1977) term structure model in the spirit of Babbs and Nowman (1999), whereas the risky asset is modelled using an affine continuous-time two-factor stochastic volatility model that extends the double Heston model of Christoffersen et al. (2009) by allowing for jumps. This state-of-the-art model captures many of the important stylized facts of (risk-free) interest rate and stock markets (see, e.g., Litterman and Scheinkman, 1991; Cont, 2001, for a discussion on important stylized facts). The interest rate term structure has many factors, capturing the level, slope, and curvature. The risky asset model has more than one volatility factor, allowing for more flexible variance dynamics; it also permits for jumps in both prices and its variance—a much-needed feature in asset price modelling (see, e.g. Bates, 1996; Eraker et al., 2003).

Mathematically speaking, we consider a continuous-time economy on the time span $\mathcal{T} = [0, T]$. The uncertainty is modelled with the probability space $(\Omega, \mathcal{F}, \mathbb{P})$ endowed with the filtration $\mathbb{F} = \{\mathcal{F}_t\}_{t\in\mathcal{T}}$ (to be formally defined later), where $\mathbb{P}$ represents the physical (real-world) measure. The risk-free asset dynamics, assumed to be the money market account and denoted by $P = \{P_t\}_{t\in\mathcal{T}}$, is given by the following equation:

$$\frac{dP_t}{P_t} = r_t\, dt, \tag{1}$$

where the short rate at time $t$ is defined by

$$r_t = \theta_r + x_{1,t} + x_{2,t} + x_{3,t}, \tag{2}$$

and

$$dx_{1,t} = -\zeta_{x_1} x_{1,t}\, dt + \sigma_{x_1}\, dW_{x_1,t}, \tag{3}$$

$$dx_{2,t} = -\zeta_{x_2} x_{2,t}\, dt + \sigma_{x_2}\, dW_{x_2,t}, \tag{4}$$

$$dx_{3,t} = -\zeta_{x_3} x_{3,t}\, dt + \sigma_{x_3}\, dW_{x_3,t}, \tag{5}$$

for which the vector $\begin{bmatrix} W_{x_1} & W_{x_2} & W_{x_3} \end{bmatrix}^\top$ is a three-dimensional standard Brownian motion with

$$d\langle W_{x_1}, W_{x_2}\rangle_t = \rho_{x_1,x_2}\, dt, \qquad d\langle W_{x_1}, W_{x_3}\rangle_t = \rho_{x_1,x_3}\, dt, \quad \text{and} \quad d\langle W_{x_2}, W_{x_3}\rangle_t = \rho_{x_2,x_3}\, dt$$

under the physical measure. We also assume that $P_0 = 1$ for convenience and without loss of generality.

We denote the risky asset price process by $S = \{S_t\}_{t\in\mathcal{T}}$, and the dynamics of this asset are given by the following stochastic differential equations (SDEs):

$$\frac{dS_t}{S_{t^-}} = \left(r_t + \xi\right) dt + \sqrt{V_{1,t^-}}\, dW_{S_1,t} + \sqrt{V_{2,t}}\, dW_{S_2,t} + dJ_{S,t}, \tag{6}$$

$$dV_{1,t} = \zeta_{V_1}\left(\theta_{V_1} - V_{1,t^-}\right) dt + \sigma_{V_1}\sqrt{V_{1,t^-}}\, dW_{V_1,t} + dJ_{V_1,t}, \tag{7}$$

$$dV_{2,t} = \zeta_{V_2}\left(\theta_{V_2} - V_{2,t}\right) dt + \sigma_{V_2}\sqrt{V_{2,t}}\, dW_{V_2,t}, \tag{8}$$

where the vector $\begin{bmatrix} W_{S_1} & W_{S_2} & W_{V_1} & W_{V_2} \end{bmatrix}^\top$ is a four-dimensional standard Brownian motion under the physical measure with

$$d\langle W_{S_1}, W_{V_1}\rangle_t = \rho_{S_1,V_1}\, dt \quad \text{and} \quad d\langle W_{S_2}, W_{V_2}\rangle_t = \rho_{S_2,V_2}\, dt,$$

while the remaining pairs of Brownian motions are independent of each other. This assumption allows our risky asset returns to be correlated with the variance dynamics, capturing the well-known leverage effect. The drift coefficient of the risky asset dynamics contains the short rate $r_t$ defined in Equation (2) and a constant, deterministic equity risk premium parameter $\xi$ for simplicity's sake. Note that the equity risk premium parameter needs to be strictly positive—investors require a higher expected return for investing in risky assets due to the greater risk of volatility and potential losses.

Both volatility factor processes allow for mean reversion and square-root diffusion; parameters $\zeta_{V_1}$ and $\zeta_{V_2}$ control the speed of mean reversion, and parameters $\theta_{V_1}$ and $\theta_{V_2}$ are the long-run values of the first and second volatility processes, respectively. The volatility of the variance parameters are denoted by $\sigma_{V_1}$ and $\sigma_{V_2}$ for the first and second processes, respectively.[5]

The risky asset jump component is defined as a compound Poisson process; that is,

$$J_{S,t} = \sum_{n=1}^{N_t} Z_{S,n},$$

where the timing of the jumps is modelled by a Poisson process $\{N_t\}_{t\in\mathcal{T}}$ with a constant intensity $\lambda$. The size of these jumps, $Z_{S,n}$, is independent and identically distributed (iid) and normally distributed with mean $\alpha$ and variance $\delta^2$.[6]

[5] The two processes $V_1$ and $V_2$ are guaranteed to stay positive, as it is commonly the case with square-root diffusions. Note that if the Feller condition is not satisfied—which is commonly the case in practice—then the processes can reach zero. If this happens, then the variance will instantly move away from zero because the diffusive term will be larger than zero at that instant.

[6] Similar return jump processes have been used by Bates (1996), Bakshi et al. (1997), Duffie et al. (2000), Pan (2002), Eraker et al. (2003), Johannes et al. (2009), Bégin (2020), among others.

Regarding variance jumps, these are also governed by a compound Poisson process

$$J_{V,t} = \sum_{n=1}^{N_t} Z_{V,n},$$

where jumps happen in both the asset price and the variance at the same time; that is, the Poisson process $\{N_t\}_{t\in\mathcal{T}}$ representing the number of jumps is the same in both Equations (6) and (7).[7] Variance jump sizes $\{Z_{V,n}\}_{n=1}^{\infty}$ are iid and exponentially distributed with mean $\nu$.[8]

The risk-free asset model is estimated using the term structure of daily US yields between 1990–2021 from the Federal Reserve System's H.15 reports. Similar to Babbs and Nowman (1999), the model is estimated using a filtering technique based on the well-known Kalman (1960) filter. Section SM.A of the Supplementary Material reports additional details on the data, the estimation methodology, and the estimated parameters.

The risky asset model is estimated using Standard & Poors 500 stock index data between 1990–2021. The estimation relies on a bootstrap particle filter in the spirit of Gordon et al. (1993) as recently implemented by Bégin et al. (2020) and Amaya et al. (2022). More details on the data, the estimation methodology, and the estimated parameters are available in Section SM.B of the Supplementary Material.

### 2.2. The mortality model

Longevity and mortality are key risks for lifetime pension pools. Guided by common sense, adding more members to a pool has a positive effect in terms of diversification (see, e.g., Bernhardt and Donnelly, 2021). Yet the potential for mortality improvements adds additional risk to the mix, reducing benefit payments for pool members.

To capture these important dimensions, we model both systematic longevity and idiosyncratic mortality risks. We propose using a stochastic mortality model that accounts for improvements in the spirit of Lee and Carter (1992) and Cairns et al. (2006). Specifically, we use a continuous-time version of a two-factor APC model that relies on the CBD-X framework (see, e.g., Dowd et al., 2020; Bégin et al., 2023b). The model produces plausible forecasts that are consistent with historical and biological trends.

#### 2.2.1. Systematic longevity risk

In this study, we rely on the following dynamics for the time-$t$ central death rate for age $x$:

$$\log\left(m_{x,t}\right) = \alpha_{\lfloor x\rfloor} + \kappa_{1,t} + \kappa_{2,t}\left(\lfloor x\rfloor - \bar{x}\right) \tag{9}$$

where $\lfloor x\rfloor$ denotes the greatest integer less than or equal to $x$ and $\bar{x}$ represents the (constant) average of the ages used in the sample. This model is a Plat (2009) variant of the well-known Cairns et al. (2006) model which allows for the addition of a nonparametric baseline age effect, $\alpha_{\lfloor x\rfloor}$.[9] We assume that the baseline age effect is constant over integer ages to mimic the behaviour of typical discrete-time models.

Once the age effect is accounted for, the remainder of the log death rates is explained by a linear function of age. The first period effect $\kappa_{1,t}$ picks up the time changes in the mortality level, and the second period effect $\kappa_{2,t}$ captures changes in the slope of the log-mortality curve from the baseline. It is well known that this assumption is justified for relatively older ages but not for younger ages (Cairns et al., 2006).

Following Plat (2009), we assume that the first period effect is modelled by a random walk and the second period effect by a mean-reverting (autoregressive) model with no drift, which are given by the following SDEs in continuous time:

$$d\kappa_{1,t} = \theta_{\kappa_1}\, dt + \sigma_{\kappa_1}\, dW_{\kappa_1,t}, \tag{10}$$

$$d\kappa_{2,t} = -\zeta_{\kappa_2}\,\kappa_{2,t}\, dt + \sigma_{\kappa_2}\, dW_{\kappa_2,t}, \tag{11}$$

where $\theta_{\kappa_1}$ is the drift of the random walk, $\zeta_{\kappa_2}$ is the speed of mean reversion, and $\sigma_{\kappa_1}$ and $\sigma_{\kappa_2}$ are variance parameters for the first and second period effects, respectively. Moreover, $\begin{bmatrix} W_{\kappa_1} & W_{\kappa_2}\end{bmatrix}^\top$ is a two-dimensional standard Brownian motion with $d\langle W_{\kappa_1}, W_{\kappa_2}\rangle_t = \rho_{\kappa_1,\kappa_2}\, dt$ under the physical measure. All mortality-related Brownian motions are mutually independent of those introduced in Section 2.1.[10,11]

The model is estimated using a filtering technique based on the Kalman (1960) filter (see Fung et al., 2017; Bégin et al., 2023b, for applications of filtering methods in the estimation of mortality modelling). We rely on US data from 1970 to 2021 for both females and males (combined) extracted from the Human Mortality Database. We consider ages from 65 to 104 in the estimation. More details on the estimation methodology, the data, and the results are available in Section SM.C.1 of the Supplementary Material.

[7] Many studies reported co-jumps in asset price and variance dynamics over the past 20 years, thus justifying our use of the same Poisson process to generate jumps in both processes (see, e.g., Pan, 2002; Eraker et al., 2003; Eraker, 2004; Jacod and Todorov, 2009; Bandi and Renò, 2016, for more details).

[8] Bates (2000), Duffie et al. (2000), Pan (2002), Eraker et al. (2003), and Todorov and Tauchen (2011) provide evidence for the presence of positive jumps in the variance process.

[9] In his paper, Plat (2009) considers a third period effect in addition to a cohort effect in his model. As we only consider older ages, this third effect is not needed here.

[10] The filtration $\mathbb{F}$ is constructed from the sigma-fields

$$\mathcal{F}_t = \sigma\left(\left\{W_{x_1,s}, W_{x_2,s}, W_{x_3,s}, W_{S_1,s}, W_{S_2,s}, J_{S,s}, W_{V_1,s}, W_{V_2,s}, J_{V,s}, W_{\kappa_1,s}, W_{\kappa_2,s}\right\}_{0\le s\le t}\right), \quad t\in\mathcal{T},$$

containing the past and present Brownian motions and jump components. It is the model filtration generated by the various stochastic processes defined in this section.

[11] Appendix A extends these simple dynamics and considers a long-memory model for the period effects in the spirit of Zhou and Li (2023).

#### 2.2.2. Idiosyncratic mortality risk

Once death rates are generated from Equation (9), we can recover survival probabilities using the following relationship:

$$ {}_sp_{x,t} = \exp\left( - \int_0^s m_{x+u,t+u}\, du \right). \tag{12} $$

These *ex post* survival probabilities can be used to generate pool members' survival and death in the context of our data generating process.[12] Specifically, we model idiosyncratic mortality risk via Bernoulli random variables as typically done in the literature. For an individual aged $x$ who is alive at time $t$, we assume that they survive until time $t+s$ with probability ${}_sp_{x,t}$ and die with probability $1 - {}_sp_{x,t}$.

## 3. Lifetime pension pool design

### 3.1. Benefits and fund dynamics of lifetime pension pools

We select a very simple structure for the dynamics of our lifetime pension pool. The pool operation is similar to that explained in Piggott et al. (2005), Qiao and Sherris (2013), and Olivieri et al. (2022) in the context of GSA plans. It is also reminiscent of the benefit update rule used by the College Retirement Equities Fund in the US and the University of British Columbia Faculty Pension Plan in Canada.

Each member brings an initial capital amount of $K$ at inception. The total pool fund then amounts to $F_0 = L_0\, K$ at time 0, where $L_0$ is the initial number of members joining the plan at inception. For simplicity, let us assume that all members joining have the same age at inception and that they are part of the same population which share similar mortality experience.

Through time, the lifetime pension pool fund changes based on investment returns, the benefits paid out to survivors, and potential death benefits. The non-guaranteed benefits, which are paid to survivors at the beginning of each period in our framework, are a function of the mortality and investment experience. In all generality, we assume that members receive $m$ payments each year, as long as they are alive.

Using typical actuarial notation, let $\ddot{a}^{(m)}_{x,t}$ denote the actuarial value at time $t$ of a whole life annuity due making $m$ payments per year of $h = \frac{1}{m}$ dollars to a member aged $x$ using the valuation basis applicable at time $t$ such that

$$ \ddot{a}^{(m)}_{x,t} = \mathrm{E}^{\mathbb{P}}\left[ \sum_{s=0}^{\infty} h\, {}_{sh}p_{x,t}\, e^{-ysh} \,\middle|\, \mathcal{F}_t \right], \tag{13} $$

where $y$ is the (continuously compounded) hurdle rate used to compute the annuity price.[13] The hurdle rate significantly impacts the annual benefits paid to retirees as shown below—a lower hurdle rate reduces the current benefit but increases the likelihood of future benefit increases, and vice versa.[14]

The total benefit amount paid by the lifetime pension pool at time $t$ is

$$ B_t = h\, \frac{F_t}{\ddot{a}^{(m)}_{x,t}} \mathbf{1}_{\{L_t \geq 1\}}, $$

where $\mathbf{1}_{\{L_t \geq 1\}}$ is the indicator function worth 1 if there is at least one member left in the pool, and zero otherwise. Each surviving member's benefit amount is therefore given by

$$ b_t = \frac{B_t}{L_t} \tag{14} $$

at time $t$ as long as the pool size is strictly positive.

We also include the possibility for a death benefit, similar to Olivieri et al. (2022). Indeed, as suggested by many (see Brown, 2009, and references therein), individuals have bequest preferences. Specifically, we assume that each of the $L_{t-h} - L_t$ members who died between $t-h$ and $t$ receives a fraction

$$ \gamma\, \frac{1}{L_{t-h}} $$

of the fund value $F_{t^-}$ at the end of the period, where $\gamma$ is a proportion of the decedent's fund value paid to their estate after the member's death, and $L_{t-h}$ is the number of survivors at time $t-h$. Just like living benefits, the amount of death benefits is not guaranteed. Additionally, while death benefits fulfil members' desires for passing on their assets, they concurrently diminish the potential for the lifetime pension pool to achieve an optimal pooling effect: the entire death benefit is retained by the pool when $\gamma = 0$, leading to the consolidation of individual longevity risks within the fund, whereas no mortality credits remain when $\gamma = 1$. We therefore expect $\gamma$ to be strictly less than one.

The pool can invest in the two assets introduced above—the risky asset $S$ and the risk-free asset $P$.[15] The allocation can be changed through time; specifically, a proportion $\omega_t$ is invested in the risky asset and $1 - \omega_t$ in the risk-free asset at the beginning of the period $[t-h, t)$, meaning that the fund dynamics can be described as follows:

[12] These are realized survival probabilities—not *ex ante* or expected probabilities—because we are explaining our data generating process here, and not the process used by the pool operator to understand risk. This important distinction will be further explained in Section 4.

[13] The annuity price of Equation (13) is calculated in semi-closed-form solution for the model of Section 2.2. See Section SM.C.2 of the Supplementary Material, Bégin et al. (2023a), and Bégin et al. (2024) for more details.

[14] In this study, we employ a constant hurdle rate that is consistent with the long-term expected returns on the investment portfolio, leading to a level expected benefit stream. A different hurdle rate could change the expected benefit stream by building potential for inflation protection, among others (Bégin and Sanders, 2023).

[15] In a robustness test, we consider long-term zero-coupon bonds as an alternative risk-free asset instead of the money market account. For more details on this test, refer to Section SM.E of the Supplementary Material.

$$F_t = \underbrace{\left(F_{t-h} - B_{t-h}\right)\left(\omega_t \frac{S_t}{S_{t-h}} + (1-\omega_t)\frac{P_t}{P_{t-h}}\right)}_{F_{t^-}}\left(1 - \gamma \frac{L_{t-h} - L_t}{L_{t-h}}\right). \tag{15}$$

As $L_{t-h} - L_t$ represents the number of decedents between time $t-h$ and $t$, the term $-\gamma F_{t^-}\frac{L_{t-h}-L_t}{L_{t-h}}$ is negative when members die (and nil otherwise) and denotes an outflow for the lifetime pension pool fund.

### 3.2. Benefit adjustments

Equation (15) is a roll-forward of the pool's fund using actual benefit and death payments as well as investment returns. Assuming that there is at least one member in the pool at time $t-h$, Equation (15) can be expressed as a function of the surviving members' benefit amount at time $t-h$:

$$\begin{aligned} F_t &= m\, b_{t-h}\, L_{t-h}\left(\ddot{a}^{(m)}_{x-h,t-h} - h\right)\left(\omega_t \frac{S_t}{S_{t-h}} + (1-\omega_t)\frac{P_t}{P_{t-h}}\right)\left(1 - \gamma \frac{L_{t-h} - L_t}{L_{t-h}}\right) \\ &= m\, b_{t-h}\, L_{t-h}\, e^{-yh}\, {}_hp_{x-h,t-h}\left(\frac{\ddot{a}^{(m)}_{x-h,t-h} - h}{e^{-yh}\, {}_hp_{x-h,t-h}}\right)\left(\omega_t \frac{S_t}{S_{t-h}} + (1-\omega_t)\frac{P_t}{P_{t-h}}\right)\left(1 - \gamma \frac{L_{t-h} - L_t}{L_{t-h}}\right). \end{aligned}$$

We can also express the fund value at time $t$ in a prospective fashion:

$$F_t = m\, b_t\, L_t\, \ddot{a}^{(m)}_{x,t} = m\, \eta_t\, b_{t-h}\, L_t\, \ddot{a}^{(m)}_{x,t},$$

where $\eta_t$ is the time-$t$ adjustment factor informed by the experience of the pool as long as members are still in the pool (i.e., $L_t \geq 1$).

Equating the retrospective and prospective values for $F_t$ and assuming the same adjustment is applied to all surviving members' benefits at time $t$ gives

$$\eta_t = \underbrace{\left(\omega_t \frac{S_t}{S_{t-h}} + (1-\omega_t)\frac{P_t}{P_{t-h}}\right)e^{-yh}}_{I_t}\underbrace{\frac{L_{t-h}\, {}_hp_{x-h,t-h}}{L_t}\mathbf{1}_{\{L_t \geq 1\}}}_{M_t}\underbrace{\frac{\ddot{a}^{(m)}_{x-h,t-h} - h}{\ddot{a}^{(m)}_{x,t}\, e^{-yh}\, {}_hp_{x-h,t-h}}}_{C_t}\underbrace{\left(1 - \gamma \frac{L_{t-h} - L_t}{L_{t-h}}\right)}_{D_t}, \tag{16}$$

where $I_t$ is the time-$t$ investment experience adjustment (IEA) factor, $M_t$ is the time-$t$ mortality experience adjustment (MEA) factor, $C_t$ is the time-$t$ changed expectation adjustment (CEA) factor, and $D_t$ is the time-$t$ death benefit experience adjustment (DBEA) factor.[16]

### 3.3. Analysis of benefit volatility with static risky asset allocation

To illustrate the benefit update rule and its impact on the benefit volatility in a simple context, we first assume that the asset allocation stays constant; that is, $\omega_t = \omega$ for all $t$. We consider $L_0 = 1{,}000$ members at inception, all aged $x = 65$ years old; each member deposits $K = \$1{,}000{,}000$ in the pool and then receives benefits at the beginning of each month (i.e., $m = 12$). The fund is invested in both risky and risk-free assets so that the unconditional annualized volatility of the investment portfolio is about 10%.[17] The pool uses a hurdle rate of 7.53% that is consistent with the expected long-run rate of return on the fund. This creates streams of benefits that are, in expectation, level. We do not consider death benefits in this first illustration (i.e., $\gamma = 0$).

We generate 100,000 investment and mortality scenarios based on the data generating process of Section 2. The top panel of Fig. 1 reports the annualized volatility of the pool's benefit adjustment. For the first 25 years or so, the benefit adjustment's volatility is about 10% and is only minimally impacted by the MEA and CEA. Indeed, virtually all of the adjustments are related to investment risk, as reported in the bottom panel of Fig. 1. After 25 years, however, the contribution of the mortality experience adjustment rises, and when members reach about 100 years old, the MEA becomes the most important contributor to the total benefit adjustment volatility. By the time members reach the age of 110—about 50 years after inception—the benefit adjustment volatility is almost exclusively impacted by the MEA. Note that the volatility of the CEA increases over time, too, but impacts the benefit volatility to some lesser extent.

## 4. Benefit volatility targeting

In this section, we explain the process in which the proportion invested in the risky asset is adjusted to target a given benefit adjustment volatility level. Indeed, the proportion $\omega_t$ can be controlled by the pool operator such that

$$\mathrm{Var}^{\mathbb{P}}\left[\eta_t \,\middle|\, \mathcal{F}_{t-h}\right] = \sigma_*^2\, h, \tag{17}$$

where $\sigma_*$ is the (annualized) exogenous volatility target. By changing its exposure to the risky asset, the pool can control the size of the benefit fluctuations. Note that the proposed update rule for $\omega_t$ is different than Olivieri et al. (2022) and Li et al. (2022), who only considered the volatility of the investment adjustment factor instead of the whole benefit payment.

In this study, the pool operator is not privy to the (assumed) data generating process—the models of Section 2—and needs to devise practical means to obtain the variance on the left side of Equation (17) via coarse assumptions and proxies. Specifically, she assumes that:

[16] Using common actuarial notation, we know that $\ddot{a}^{(m)}_{x-h} = h + e^{-yh}\, {}_hp_{x-h}\ddot{a}^{(m)}_x$ when mortality is deterministic (see, e.g., Piggott et al., 2005). This relationship, however, is not satisfied for stochastic mortality models, meaning that $C_t$ will only equal one if there are no changes to future mortality expectations.

[17] Investing 56.8% of the pool's assets in the risky asset and the rest in the risk-free asset yields an unconditional annualized volatility of about 10%.

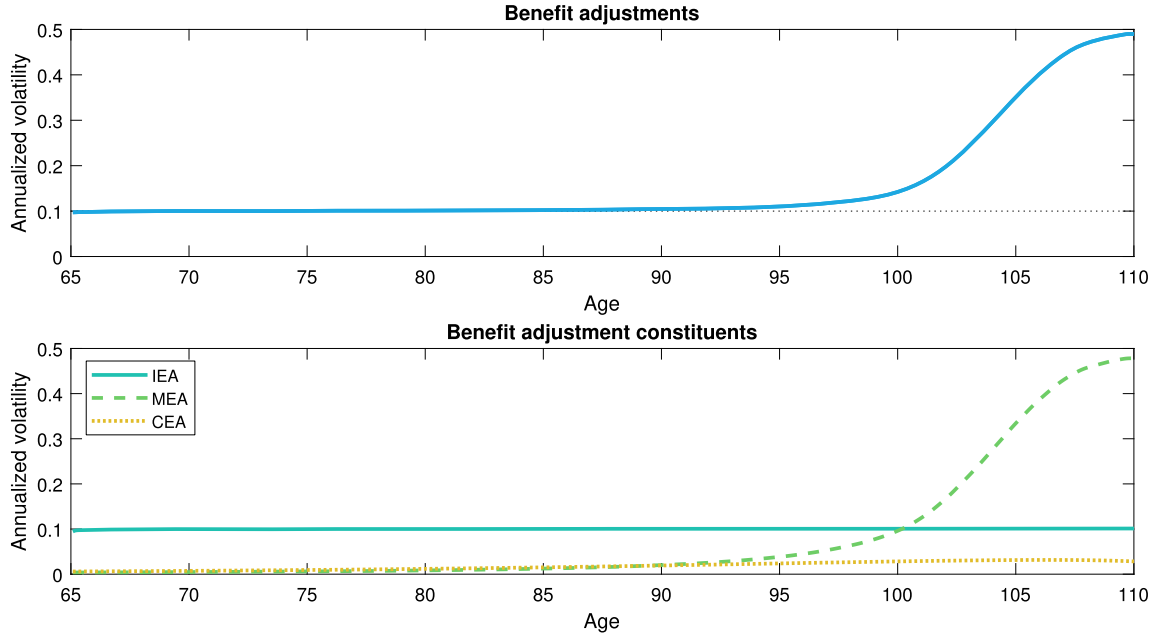


**Fig. 1. Annualized volatility of the benefit adjustments and its constituents for a static allocation in the risky asset**. *Notes:* This figure shows the annualized volatility of the benefit adjustments (top panel) as well as its constituents (bottom panel) between ages 65 and 110; that is, the investment experience adjustment (IEA), the mortality experience adjustment (MEA), and the changed expectation adjustment (CEA). The pool has 1,000 members at inception. It invests 56.8% of its assets in the risky asset, and the remainder in the risk-free asset; this corresponds to an unconditional annualized volatility of about 10%. The simulation begins in January 2022. This example does not include death benefits (i.e., $\gamma = 0$), so there is no adjustment related to this component.

- The mortality table is static and based on time $t-h$ information. In other words, the CEA adjustment factor is assumed to be one and the survival probability over the next period is given by ${}_h\tilde{p}_{x-h,t-h} = \mathrm{E}^{\mathbb{P}}\left[{}_hp_{x-h,t-h} \,\middle|\, \mathcal{F}_{t-h}\right]$.
- The number of pool members at time $t$ conditional on information at time $t-h$ is given by a binomial distribution with size parameter $L_{t-h}$ and probability parameter ${}_h\tilde{p}_{x-h,t-h}$.
- The time-$t$ risk-free asset price $P_t$ based on the information at time $t-h$ is given by

$$P_t = P_{t-h}\, e^{\hat{r}_t h},$$

where $\hat{r}_t$ is proxied by the three-month zero-coupon bond yield observed at time $t-h$.
- The time-$t$ risky asset price $S_t$ based on the information at time $t-h$ is given by

$$S_t = S_{t-h}\, e^{\varepsilon_t}, \tag{18}$$

where $\varepsilon_t$ is normally distributed with mean parameter $\left(\hat{r}_t + \hat{\xi} - \frac{\hat{\sigma}_t^2}{2}\right)h$ and variance parameter $\hat{\sigma}_t^2 h$. Parameter $\hat{\xi}$ is set to the (annualized) sample average equity risk premium based on the risky asset returns. Parameter $\hat{\sigma}_t^2$ is obtained via nonparametric volatility forecasting methods based on high-frequency returns and information up to time $t-h$ (see Section 4.1 for more details).

Let $\tilde{I}_t$, $\tilde{M}_t$, $\tilde{C}_t$, and $\tilde{D}_t$ be the pool operator's proxies for $I_t$, $M_t$, $C_t$, and $D_t$, respectively. As a result of the pool operator's exogenous target $\sigma_*^2$, we have that

$$\begin{aligned}\sigma_*^2 h &= \mathrm{Var}\left[\tilde{I}_t\, \tilde{M}_t\, \tilde{C}_t\, \tilde{D}_t \,\middle|\, L_{t-h},\, {}_h\tilde{p}_{x-h,t-h}, \hat{r}_t, \hat{\sigma}_t\right] \\ &= \mathrm{E}\left[\tilde{I}_t^2 \,\middle|\, \hat{r}_t, \hat{\sigma}_t\right] \mathrm{E}\left[\tilde{M}_t^2\, \tilde{D}_t^2 \,\middle|\, L_{t-h},\, {}_h\tilde{p}_{x-h,t-h}\right] - \mathrm{E}\left[\tilde{I}_t \,\middle|\, \hat{r}_t, \hat{\sigma}_t\right]^2 \mathrm{E}\left[\tilde{M}_t\, \tilde{D}_t \,\middle|\, L_{t-h},\, {}_h\tilde{p}_{x-h,t-h}\right]^2 \end{aligned} \tag{19}$$

because $\tilde{C}_t = 1$ and both $\tilde{M}_t$ and $\tilde{D}_t$ are correlated as they depend on $L_t$.

### 4.1. Moments of the investment adjustment factor

For the variance related to investment returns, we use a volatility-forecasting methodology that relies on realized volatility and high-frequency returns. Corsi (2009) showed that a simple HAR model combined with realized volatility statistics produces excellent forecasting performance.[18] The basic HAR framework of Corsi has been extended in many directions over the past decade (see, e.g., Andersen et al., 2007; Busch et al., 2011; Corsi and Renò, 2012, among others).

In this study, we rely on a simple implementation similar to that of Corsi (2009) and Corsi and Renò (2012) which includes the realized volatility and the leverage effect via the inclusion of negative returns over different horizons. Specifically, we have that

[18] The volatility forecasting step is important because it could also significantly improve portfolio returns (see, e.g., Mylnikov, 2021).

**Table 1**
Heterogeneous autoregressive model parameters for volatility forecasts.

| Parameter | Estimate | Standard error |
|---|---|---|
| $\chi$ | 0.0292 | (0.0011) |
| $\beta^{(\mathrm{d})}$ | 0.2142 | (0.0141) |
| $\beta^{(\mathrm{w})}$ | 0.3240 | (0.0205) |
| $\beta^{(\mathrm{m})}$ | 0.2110 | (0.0163) |
| $\gamma^{(\mathrm{d})}$ | -0.6902 | (0.0803) |
| $\gamma^{(\mathrm{w})}$ | -1.6248 | (0.2692) |
| $\gamma^{(\mathrm{m})}$ | 2.0637 | (0.5531) |
| Error variance | 0.0018 | |
| $R^2$ | 0.6353 | |

*Notes:* This table reports the parameters of the HAR model used at the inception of the pool. These linear regression parameters are obtained by using the least squares method. Note that these parameters are updated along each future path, meaning that new path-specific information is incorporated in the estimates, which are reestimated for all scenarios and each month.

$$\hat{\sigma}_t = \chi + \beta^{(\mathrm{d})}\,\mathrm{RVol}^{(1)}_{t-h} + \beta^{(\mathrm{w})}\,\mathrm{RVol}^{(5)}_{t-h} + \beta^{(\mathrm{m})}\,\mathrm{RVol}^{(21)}_{t-h} + \gamma^{(\mathrm{d})}\,r^{(1)}_{t-h} + \gamma^{(\mathrm{w})}\,r^{(5)}_{t-h} + \gamma^{(\mathrm{m})}\,r^{(21)}_{t-h} + \epsilon_t,$$

where

- the dependent variable $\hat{\sigma}_t$ is the (annualized) volatility between time $t-h$ and $t$, which is proxied by the total realized volatility between time $t-h$ and $t$,
- the regressors $\mathrm{RVol}^{(1)}_{t-h}$, $\mathrm{RVol}^{(5)}_{t-h}$, and $\mathrm{RVol}^{(21)}_{t-h}$ are the (annualized) past day, week, and month realized volatilities—proxies for the square root of the quadratic variation of the risky asset price process—respectively, defined as

$$\mathrm{RVol}^{(q)}_{t-h} = \sqrt{\frac{1}{q}\sum_{i=0}^{q-1}\mathrm{RV}_{t-h-i/252}},$$

  and $\mathrm{RV}_t$ is the daily realized variance for the day ending at time $t$,
- the regressors $r^{(\mathrm{d})}_{t-h}$, $r^{(\mathrm{w})}_{t-h}$, and $r^{(\mathrm{m})}_{t-h}$ are the past day, week, and month leverage effect—proxied by the negative part of the observed returns—respectively, defined as

$$r^{(q)}_{t-h} = \min\left(0, \frac{1}{q}\sum_{i=0}^{q-1}\log\left(\frac{S_{t-h-q/252}}{S_{t-h-(q+1)/252}}\right)\right),$$

  and
- the unobserved random variable $\epsilon_t$ adds noise to the linear relationship between the dependent variable and regressors.[19]

This model works well and produces reliable estimates of the future volatility. Table 1 reports the parameters of the HAR model used at the inception of the pool. These linear regression parameters are obtained by using the least squares method; they are consistent with those obtained in other studies in the literature and with financial intuition. The future volatility is positively related to the last day, week, and month's volatility (i.e., $\beta^{(\mathrm{d})}$, $\beta^{(\mathrm{w})}$, and $\beta^{(\mathrm{m})}$ are positive). Recent negative returns tend to increase the future volatility; yet more distant negative returns make the future volatility lower, which is consistent with arguments of mean reversion—a well-known stylized fact of market volatility.[20] The coefficient of determination obtained from the HAR model is very high, with a value of about 64%, leading to reliable volatility forecasts. Note that these parameters are updated along each future path, meaning that new information is incorporated in the estimates after inception.[21]

Once the value of $\hat{\sigma}_t$ is found, we can then use it to calculate the first two moments of $\tilde{I}_t$. Using the approximation of Equation (18), we obtain the moments as follows.

**Proposition 1.** *The first two moments of the investment experience adjustment approximation are given by*

$$\mathrm{E}\left[\tilde{I}_t \,\middle|\, \hat{r}_t, \hat{\sigma}_t\right] = e^{(\hat{r}_t - y)h}\left(\omega_t\left(e^{\hat{\xi}h} - 1\right) + 1\right),$$

$$\mathrm{E}\left[\tilde{I}_t^2 \,\middle|\, \hat{r}_t, \hat{\sigma}_t\right] = e^{2(\hat{r}_t - y)h}\left(\omega_t^2\left(e^{\left(2\hat{\xi}+\hat{\sigma}_t^2\right)h} - 2e^{\hat{\xi}h} + 1\right) + \omega_t\left(2e^{\hat{\xi}h} - 2\right) + 1\right).$$

**Proof.** See Section SM.D.1 of the Supplementary Material. □

[19] The realized variance estimates are computed from high-frequency returns observed every five minutes throughout each day; these returns are obtained via Tick Data. This study relies on estimates computed using the subsampling methodology of Zhang et al. (2005) from S&P 500 intraday returns. The leverage effect variables are computed from daily returns obtained from Compustat.

[20] Negative returns are typically tied to increases in the spot volatility—a stylized fact known as Black's leverage effect in finance. Yet, over longer horizons, past increases in volatility tend to also be accompanied by future decreases via mean reversion of the volatility process.

[21] After inception, the estimates of Table 1 vary at each time step and based on each path's information—mimicking the process used by the pool operator to update the model parameters based on the most recent data available.

### 4.2. Moments of the mortality and death benefit adjustment factors

In our setting, we assume that the pool operator has access to a static mortality table that includes a mortality improvement scale to capture mortality improvement—consistent with the data used to estimate the data generating process and the information available at time $t-h$ along each path. This information is used to compute the moments of the mortality and death benefit adjustment factors. Indeed, the product of $\tilde{M}_t$ and $\tilde{D}_t$ can be simplified:

$$\tilde{M}_t\,\tilde{D}_t = \left(\frac{L_{t-h}}{L_t}\,{}_h\tilde{p}_{x-h,t-h}\,(1-\gamma) + {}_h\tilde{p}_{x-h,t-h}\,\gamma\right)\mathbf{1}_{\{L_t\geq 1\}},$$

which involves the reciprocal of $L_t$. The first two moments associated with this random variable can be expressed via generalized hypergeometric functions.

**Proposition 2.** *The first two moments of the mortality and death benefit experience adjustment approximations are given by:*

$$\begin{aligned}
\mathrm{E}\left[\tilde{M}_t\,\tilde{D}_t\,\middle|\,L_{t-h},\,{}_h\tilde{p}_{x-h,t-h}\right] &= L_{t-h}^2\,{}_h\tilde{p}_{x-h,t-h}^2\,(1-\gamma)\left(1-{}_h\tilde{p}_{x-h,t-h}\right)^{L_{t-h}-1}{}_3F_2\left(\{1,1,1-L_{t-h}\},\{2,2\};\frac{-{}_h\tilde{p}_{x-h,t-h}}{1-{}_h\tilde{p}_{x-h,t-h}}\right)\\
&\quad + {}_h\tilde{p}_{x-h,t-h}\,\gamma\left(1-\left(1-{}_h\tilde{p}_{x-h,t-h}\right)^{L_{t-h}}\right),\\
\mathrm{E}\left[\tilde{M}_t^2\,\tilde{D}_t^2\,\middle|\,L_{t-h},\,{}_h\tilde{p}_{x-h,t-h}\right] &= L_{t-h}^3\,{}_h\tilde{p}_{x-h,t-h}^3\,(1-\gamma)^2\left(1-{}_h\tilde{p}_{x-h,t-h}\right)^{L_{t-h}-1}{}_4F_3\left(\{1,1,1,1-L_{t-h}\},\{2,2,2\};\frac{-{}_h\tilde{p}_{x-h,t-h}}{1-{}_h\tilde{p}_{x-h,t-h}}\right)\\
&\quad + 2L_{t-h}^2\,{}_h\tilde{p}_{x-h,t-h}^3\,(1-\gamma)\,\gamma\left(1-{}_h\tilde{p}_{x-h,t-h}\right)^{L_{t-h}-1}{}_3F_2\left(\{1,1,1-L_{t-h}\},\{2,2\};\frac{-{}_h\tilde{p}_{x-h,t-h}}{1-{}_h\tilde{p}_{x-h,t-h}}\right)\\
&\quad + {}_h\tilde{p}_{x-h,t-h}^2\,\gamma^2\left(1-\left(1-{}_h\tilde{p}_{x-h,t-h}\right)^{L_{t-h}}\right),
\end{aligned}$$

*where* ${}_pF_q(\{a_1,\ldots,a_p\},\{b_1,\ldots,b_q\};z)$ *is the generalized hypergeometric function (see Andrews et al., 1999, for more details on this function).*

**Proof.** See Section SM.D.2 of the Supplementary Material. □

### 4.3. Volatility-targeting-based allocation

Based on Propositions 1 and 2, the pool operator can now solve Equation (19) in closed form using her coarse assumptions.

**Proposition 3.** *Based on the information available to the pool operator, Equation* (19) *yields the following volatility-targeting allocation:*

$$\omega_t = \begin{cases} \frac{-b+\sqrt{b^2-4ac}}{2a} & \text{if } b^2\geq 4ac \\ 0 & \text{otherwise} \end{cases}, \tag{20}$$

*where*

$$\begin{aligned}
a &= \mathrm{E}\left[\tilde{M}_t^2\,\tilde{D}_t^2\,\middle|\,L_{t-h},\,{}_h\tilde{p}_{x-h,t-h}\right]\left(e^{\left(2\hat{\xi}+\hat{\sigma}_t^2\right)h}-2e^{\hat{\xi}h}+1\right)-\mathrm{E}\left[\tilde{M}_t\,\tilde{D}_t\,\middle|\,L_{t-h},\,{}_h\tilde{p}_{x-h,t-h}\right]^2\left(e^{2\hat{\xi}h}-2e^{\hat{\xi}h}+1\right),\\
b &= \mathrm{E}\left[\tilde{M}_t^2\,\tilde{D}_t^2\,\middle|\,L_{t-h},\,{}_h\tilde{p}_{x-h,t-h}\right]\left(2e^{\hat{\xi}h}-2\right)-\mathrm{E}\left[\tilde{M}_t\,\tilde{D}_t\,\middle|\,L_{t-h},\,{}_h\tilde{p}_{x-h,t-h}\right]^2\left(2e^{\hat{\xi}h}-2\right),\\
c &= \mathrm{E}\left[\tilde{M}_t^2\,\tilde{D}_t^2\,\middle|\,L_{t-h},\,{}_h\tilde{p}_{x-h,t-h}\right]-\mathrm{E}\left[\tilde{M}_t\,\tilde{D}_t\,\middle|\,L_{t-h},\,{}_h\tilde{p}_{x-h,t-h}\right]^2-\sigma_*^2\,h\,e^{2(y-\hat{r}_t)h}.
\end{aligned}$$

**Proof.** See Section SM.D.3 of the Supplementary Material. □

Generally speaking, the quadratic equation has two roots; in our application, when these roots are real, one tends to be positive and the other negative. We only focus on the positive root because we wish to capture the equity risk premium; indeed, a negative allocation—shorting the risky asset to buy the risk-free asset—would give a negative return, on average, and lead to an inefficient allocation.

It is also possible that the quadratic equation has no real solution, in which case we set $\omega_t$ to zero. This happens in cases when it is impossible to reduce the allocation to match perfectly the target volatility because the risk associated with mortality is larger than the target. In other words, when the target cannot be reached, then the second best option for the pool operator is to choose her allocation so that it minimizes the level of benefit risk.

Fig. 2 shows the impact of the forecast annualized volatility $\hat{\sigma}_t$, the pool size, and the survival probability on the risky asset allocation of Equation (20) for a fixed volatility target. As expected, the allocation increases when the forecast volatility is lower—a common relationship in the context of volatility targeting. The size of the pool impacts the allocation when the survival probability tends to be lower: as the survival probability is lower for older individuals, we observe a lower allocation to the risky asset for a smaller pool with older members (which already has significant volatility due to mortality) than for a larger pool with the same members (where the mortality risk has been diversified).

## 5. Implementation of the strategy

This section presents the results in simple contexts—with and without death benefits. We also consider some robustness tests by changing the exogenous volatility target and the size of the pool at inception.

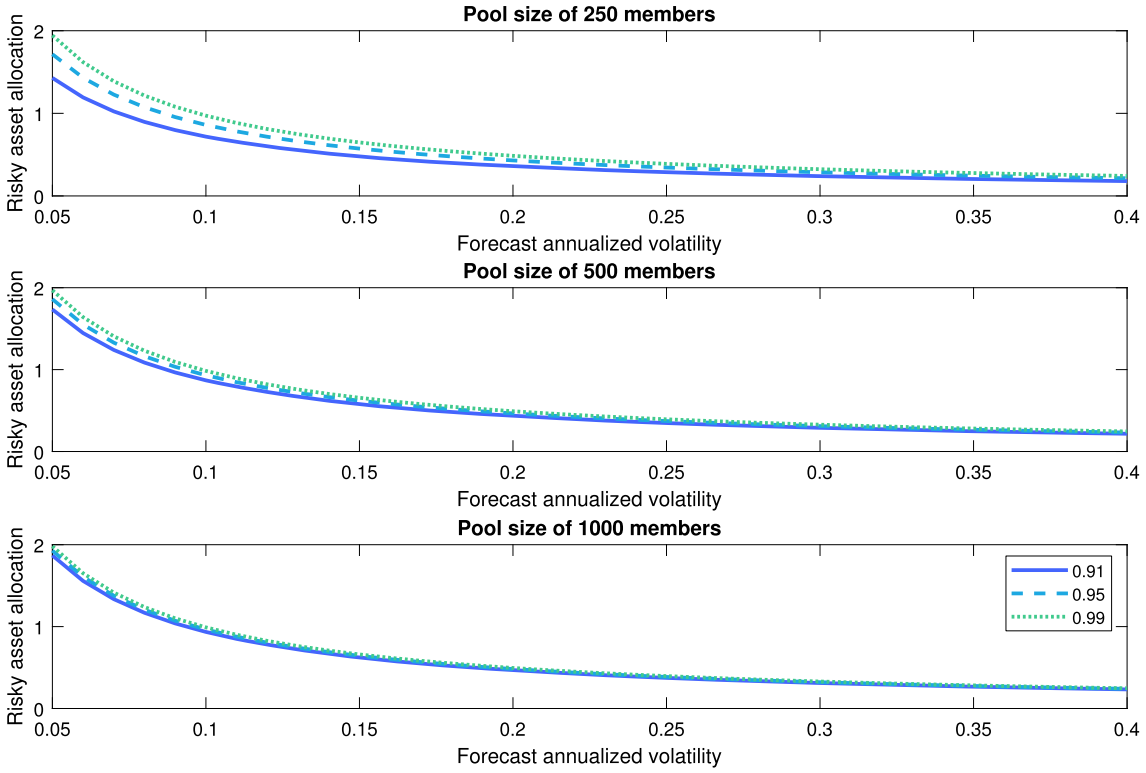


**Fig. 2. Risky asset allocation as a function of the forecast annualized volatility, the pool size, and the survival probability**. *Notes:* This figure shows the impact of the forecast annualized volatility, the pool size, and the survival probability on the risky asset allocation of Equation (20) for a fixed (annualized) volatility target of 10%. We consider pool sizes of 250 (top panel), 500 (middle panel), and 1000 members (bottom panel) as well as survival probabilities of 0.91 (solid line), 0.95 (dashed line), and 0.99 (dotted line).

### *5.1. Comparison with static allocations*

Similar to Section 3.3, we consider a pool of 1,000 members at inception, all aged $x = 65$ years old. They each deposit $K = \$1{,}000{,}000$ in the pool and receive monthly benefits at the beginning of each month. The fund is invested, again, in both risky and risk-free assets. The allocation to the risky asset changes every month based on the rule set forth in Proposition 3; the exogenous volatility target $\sigma_*$ is set to 10%. The hurdle rate is set to the same value used in Section 3.3—a value consistent with the expected long-run rate of the fund return under the static case. We do not consider death benefits in this illustration (i.e., $\gamma = 0$).

For each scenario, we compute the fund value, risky asset allocation, benefits, and their associated adjustments (IEA, MEA, CEA, and DBEA) recursively for the static strategy and the volatility-targeting strategy also called dynamic allocation throughout this article. Fig. 3 provides a visual representation of these variables for a representative scenario. The fund value (top-left panel of Fig. 3) naturally decreases over time as benefits are disbursed to members, aligning with our expectations. The top-right panel of Fig. 3 illustrates how the allocation to the risky asset fluctuates based on factors such as the pool size, survival probability, and forecast volatility of the risky asset for the next month. Notably, the allocation decreases when the pool size and survival probability are low or when the forecast volatility is high, as previously discussed in Fig. 2. During the initial 30 years, changes in volatility predominantly influence the allocation. However, as time progresses beyond this period, the allocation to the risky asset tends to decrease, coinciding with the ageing of the pool and its members.

The annualized benefits (middle-left panel of Fig. 3), expressed in thousands of dollars throughout this article, exhibit variations driven by investment returns, idiosyncratic mortality within the pool, and systematic longevity resulting from changed expectation in the population. The investment experience adjustments (middle-right panel of Fig. 3) are directly influenced by the asset allocation. Notably, the IEA tends to display greater stability when the allocation to the risky asset decreases, and conversely, it becomes more volatile with increased allocation to the risky asset. This outcome notably *chops* the tails of the distribution—a by-product of the reduced risky asset allocation during periods of heightened market volatility.

The mortality experience adjustments and the changed expectation adjustments to a lesser extent (bottom-left and bottom-right panels of Fig. 3, respectively) grow in magnitude over time as the pool ages. This development is expected because older members are statistically more likely to die, intensifying the uncertainty surrounding mortality gains for surviving members. The MEA and CEA are identical in both dynamic and static asset allocation cases.

Building on the intuition of Fig. 3, we now turn to summaries of our 100,000 scenarios. Fig. 4 reports the funnels of doubt for the risky asset allocation, defined as average values (solid lines) as well as $5^{\text{th}}$ and $95^{\text{th}}$ percentiles (dashed lines) of the monthly distribution of $\omega_t$. We consider, again, static and dynamic allocation strategies. On the one hand, the static allocation leads to a constant weight of 56.8% for all scenarios by design. The dynamic allocation strategy, on the other hand, displays a certain level of uncertainty. The average allocation for the dynamic strategy is higher than the static allocation during the first 30 years (i.e., 69.7% versus 57.3%), leading to additional returns, on average. During this period, there are also sizeable variations in the allocation: the $5^{\text{th}}$ and $95^{\text{th}}$ percentiles of the risky asset allocation are 38.1% and 116.8%, respectively. Then, after the initial 30 years, the average allocation obtained from the dynamic strategy decreases because of the increased risk in the MEA and CEA; the funnel also becomes narrower around the mean value, to finally reach a risky asset allocation of zero in all scenarios.

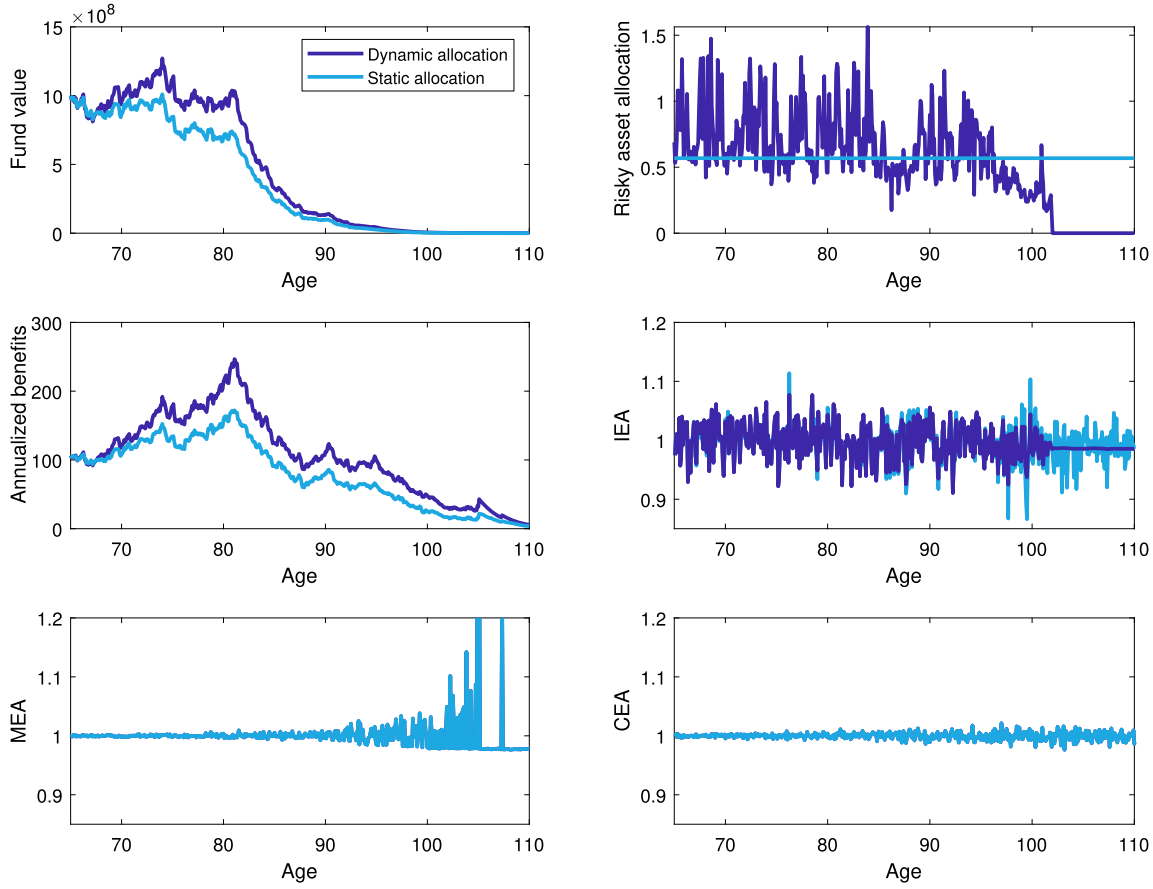


**Fig. 3. Illustrative example of the fund value, risky asset allocation, benefits, and benefit adjustment constituents for a given scenario**. *Notes:* This figure shows an illustrative example of the fund value, risky asset allocation, (annualized) benefits in thousands of dollars, and adjustment constituents for a given scenario. IEA stands for investment experience adjustment, MEA for mortality experience adjustment, and CEA for changed expectation adjustment. In this scenario, the death benefit parameter $\gamma$ is set to zero, so DBEA is nil.

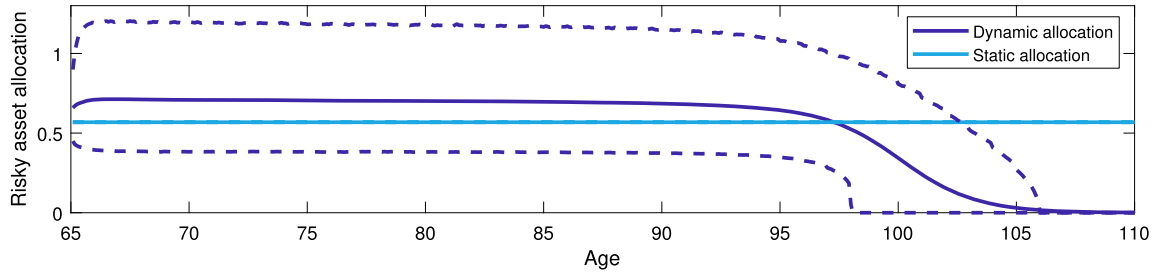


**Fig. 4. Risky asset allocation funnels of doubt for dynamic and static asset allocation**. *Notes:* This figure shows funnels of doubt for the risky asset allocation $\omega_t$. We consider dynamic and static allocation along with the basic setting of Section 5. Average values (solid lines) as well as $10^{\text{th}}$ and $90^{\text{th}}$ percentiles (dashed lines) are reported. Note that the static allocation strategy is constant through time, hence leading to a degenerate funnel at 56.8%.

Fig. 5 presents funnels of doubt for annualized benefits. Consistent with a higher average risky asset allocation when using a dynamic strategy, the average benefit is higher than that of the static strategy. Indeed, the static allocation leads to a level average as discussed in Section 3.3, whereas the dynamic allocation average benefit increases for the first 30–35 years. Furthermore, the $5^{\text{th}}$ and $95^{\text{th}}$ percentiles of the volatility-targeting strategy's benefit distribution consistently surpass those of the static strategy, resulting in superior benefits, generally speaking. This outcome is a direct consequence of the strategy's design, which involves reducing the allocation to the risky asset during periods of heightened volatility. This, in turn, lowers the likelihood of significant drawdowns and improves the left tail of the benefit distribution.

Panel A of Table 2 complements the information presented in Fig. 5 by offering a detailed view of the annualized benefit distribution for specific ages (i.e., 75, 85, 95, and 105 years old); it provides a comprehensive set of summary statistics and key percentiles for these age groups and for the two strategies. Across all scenarios, the benefits derived from dynamic volatility-targeting allocations consistently outperform those of static allocations. For instance, at age 75, the dynamic allocation yields larger benefits in 88.2% of the scenarios. This trend continues, with 95.0% at age 85 and 97.5% at age 95.

As we approach the end of the time horizon, the average benefit of the dynamic allocation strategy experiences a decline. This reduction can be attributed to the fact that, in virtually all cases, the risky asset allocation approaches zero towards the end of the investment horizon.

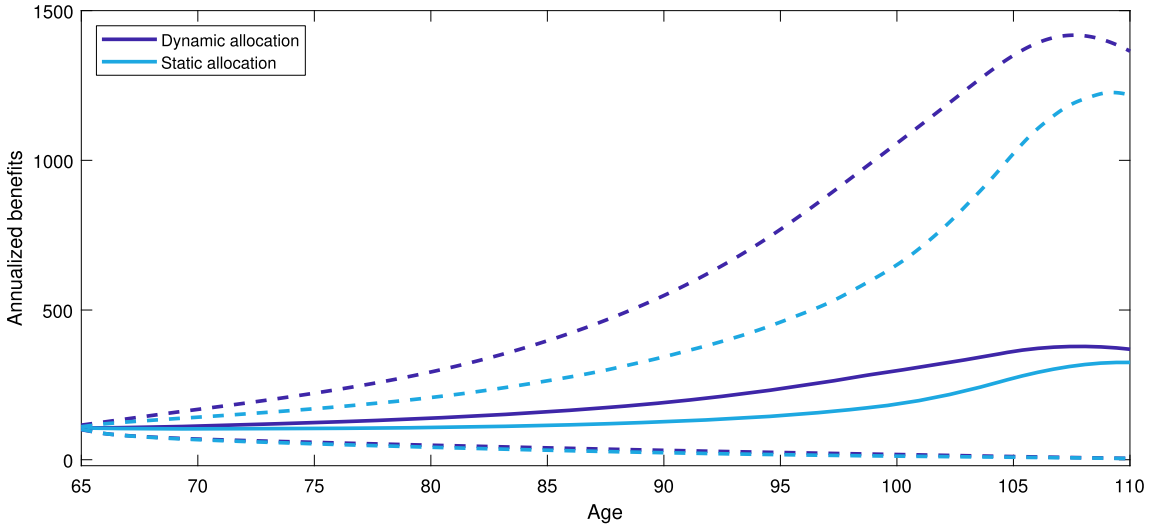


**Fig. 5. Annualized benefits funnels of doubt for dynamic and static asset allocations**. *Notes:* This figure reports funnels of doubt for the annualized benefits in thousands of dollars. We consider dynamic and static allocation strategies along with the basic setting of Section 5. Average values (solid lines) as well as 5$^{th}$ and 95$^{th}$ percentiles (dashed lines) are reported.

**Table 2**
Summary statistics of benefits and benefit adjustments.

| **Panel A: Summary statistics of benefits** | | | | | | | | |
|---|---|---|---|---|---|---|---|---|
| | 75 | | 85 | | 95 | | 105 | |
| | Dynamic | Static | Dynamic | Static | Dynamic | Static | Dynamic | Static |
| Average | 123.7 | 104.4 | 159.4 | 114.4 | 235.7 | 146.7 | 359.7 | 269.9 |
| Standard deviation | 51.6 | 36.1 | 124.7 | 78.2 | 335.2 | 187.9 | 1046.1 | 775.5 |
| 5$^{th}$ percentile | 58.3 | 53.3 | 39.7 | 32.0 | 24.2 | 17.1 | 10.7 | 8.3 |
| 25$^{th}$ percentile | 86.8 | 78.9 | 78.3 | 61.5 | 67.3 | 46.1 | 44.4 | 34.3 |
| Median | 114.5 | 100.2 | 125.8 | 95.0 | 135.7 | 90.3 | 120.0 | 91.5 |
| 75$^{th}$ percentile | 150.3 | 125.5 | 200.3 | 144.7 | 277.4 | 176.5 | 323.9 | 245.0 |
| 95$^{th}$ percentile | 220.8 | 169.8 | 392.3 | 261.4 | 758.0 | 454.8 | 1363.8 | 1015.8 |
| Proportion (%) | 88.2 | 11.8 | 95.0 | 5.0 | 97.5 | 2.5 | 79.6 | 20.4 |
| **Panel B: Summary statistics of benefit adjustments** | | | | | | | | |
| | 75 | | 85 | | 95 | | 105 | |
| | Dynamic | Static | Dynamic | Static | Dynamic | Static | Dynamic | Static |
| Average | 1.001 | 1.000 | 1.002 | 1.001 | 1.002 | 1.001 | 1.004 | 1.009 |
| Standard deviation | 0.107 | 0.100 | 0.107 | 0.102 | 0.107 | 0.109 | 0.326 | 0.343 |
| 5$^{th}$ percentile | 0.950 | 0.951 | 0.950 | 0.951 | 0.950 | 0.949 | 0.953 | 0.930 |
| 25$^{th}$ percentile | 0.983 | 0.984 | 0.983 | 0.984 | 0.982 | 0.982 | 0.966 | 0.964 |
| Median | 1.003 | 1.001 | 1.003 | 1.002 | 1.002 | 1.001 | 0.976 | 0.987 |
| 75$^{th}$ percentile | 1.022 | 1.017 | 1.022 | 1.018 | 1.022 | 1.020 | 1.004 | 1.021 |
| 95$^{th}$ percentile | 1.049 | 1.045 | 1.050 | 1.047 | 1.051 | 1.051 | 1.138 | 1.149 |
| Proportion (%) | 56.3 | 43.7 | 56.5 | 43.5 | 54.7 | 45.3 | 41.1 | 58.9 |

*Notes:* This table reports summary statistics of benefits and monthly benefit adjustments for four ages of interest (75, 85, 95, and 105 years old) and for the two allocation strategies. We consider the basic setting of Section 5. The proportion value for the dynamic case reports the proportion of scenarios with a higher value of benefit (or benefit adjustment) for the dynamic strategy when compared to the static case. The proportion value for the static case is the opposite.

Consequently, the portfolio's returns fall below the hurdle rate, resulting in relatively minor benefit reductions, on average. This decrease in returns is accompanied by a reduction in risk, particularly evident in the left tail of the benefit distribution. For instance, the 5$^{th}$ percentile of annualized benefits for members aged 105 is $10,700 with the dynamic strategy, compared to $8,300 with the static strategy. Furthermore, it is worth noting that in 79.6% of the scenarios, the dynamic allocation strategy yields higher benefits for members aged 105. This underscores the effectiveness of the dynamic approach in achieving favourable outcomes, even in the later stages of the investment horizon.

The top panel of Fig. 6 and Panel B of Table 2 provide insights into monthly benefit adjustments. During the initial 30 years, both the average and median benefit adjustments are notably higher for the dynamic strategy, contributing to the observed steady increase in the average benefits in Fig. 5. In general, the dynamic strategy exhibits larger adjustments when compared to the static approach. However, beyond the initial 35 years, the dynamic allocation tends to yield lower average adjustments compared to the static approach—traded for a thinner left tail of the adjustment distribution. This effectively reduces the severity of drastic decreases, resulting in an overall lower risk profile for this strategy.

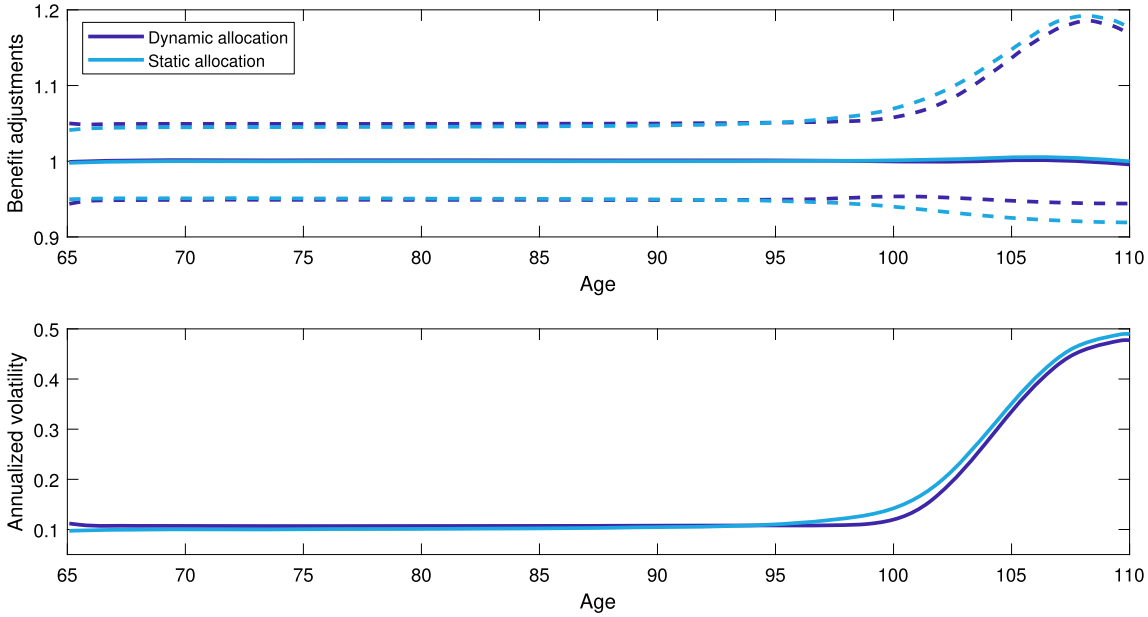


**Fig. 6. Benefit adjustment funnels of doubt and annualized volatility of the benefit adjustments for dynamic and static asset allocations**. *Notes:* The top panel of this figure shows funnels of doubt for the benefit adjustments, whereas the bottom panel reports the annualized volatility of the benefit adjustments. We consider dynamic and static allocation strategies along with the basic setting of Section 5. Average values (solid lines) as well as 5$^{th}$ and 95$^{th}$ percentiles (dashed lines) are reported in the top panel.

The annualized benefit adjustment volatility is depicted in the bottom panel of Fig. 6. In general, for both methods, it remains in the neighbourhood of the 10% target during the initial 30 years. However, the dynamic strategy distinguishes itself from the static strategy by maintaining the overall adjustment volatility close to 10% for an additional five years, achieved through a reduction in the allocation to the risky asset during this period as illustrated in Fig. 4. Beyond the initial 35 years, the mortality-related adjustments—MEA and CEA—tend to increase, resulting in challenges for sustaining the benefit adjustment volatility near its target. That being said, it is still systematically lower than that implied by the static strategy, thus leading to less variability in the benefit stream.

### 5.2. Implications of death benefits

In the previous subsection, we established a baseline scenario by setting the death benefit parameter $\gamma$ to zero. In the current analysis, we explore the influence of varying this parameter on the dynamic strategy's outcomes. The left panels of Fig. 7 show the annualized benefits funnels of doubt for a death benefit parameter of 25% (top panel) and 75% (bottom panel).[22] The dynamic strategy's superiority in terms of generating higher benefits holds true even when death benefits are introduced: the funnels of doubt generated from the dynamic allocation systematically outperform those of the static strategy. This conclusion is further supported by Table 3: the stream obtained with the dynamic strategy leads to more benefits. Furthermore, in about 90% of the scenarios, the dynamic allocation improves the benefits obtained by members, and this for all ages considered in the table.

The right panels of Fig. 7 present monthly benefit adjustments funnels of doubt.[23] Similar to what we observed in Fig. 6, the dynamic allocation leads to higher average adjustments for the initial 30–35 years. Beyond this period, the adjustments for the dynamic allocation are slightly lower than those obtained with the static strategy, but the risk—especially in the left tail of the benefit adjustments—is greatly reduced, contributing to more stable outcomes.

### 5.3. Impact of the exogenous volatility target

The volatility target could influence the results presented in Section 5.1, so we assess the repercussions of changing this assumption. We consider two distinct volatility targets: 13% and 16%.

Fig. 8 mirrors Fig. 4 and shows funnels of doubt for the risky asset allocation. Indeed, these funnels of doubt closely resemble those presented in the baseline case of Section 5.1. Yet the allocation to the risky asset tends to increase as we raise the target. For instance, the 95$^{th}$ percentile of the risky asset allocation in the dynamic case when the target is 13% (16%) is about 160% (200%).

The combination of increased allocations to the risky asset and the timing of these changes—smaller allocation when volatility is high and vice versa—lead to notable enhancements in the benefit streams, as shown in Table 4.[24] Once again, the dynamic strategy consistently delivers robust benefit streams that outperform those generated by the static allocation strategy in approximately 90% of the scenarios.

[22] In this application, we maintain a constant hurdle rate of 7.53%, which results in declining benefits in the static case. It is important to recognize that the overall behaviour of the benefit stream could exhibit an upward trend by using a lower hurdle rate as done in Olivieri et al. (2022), and our findings remain robust to changes in this assumption.

[23] See Table SM.5 of the Supplementary Material for more details on the monthly benefit adjustments with non-zero death benefits.

[24] The interested reader can refer to summary statistics about the benefit adjustments with different volatility targets in Table SM.6 of the Supplementary Material.

**Table 3**
Summary statistics of benefits with death benefits.

| **Panel A: Summary statistics of benefits for a death benefit parameter of 25%** | | | | | | | | |
|---|---|---|---|---|---|---|---|---|
| | 75 | | 85 | | 95 | | 105 | |
| | Dynamic | Static | Dynamic | Static | Dynamic | Static | Dynamic | Static |
| Average | 117.5 | 99.1 | 134.4 | 96.2 | 147.0 | 90.4 | 124.3 | 82.1 |
| Standard deviation | 49.1 | 34.2 | 105.0 | 65.6 | 209.1 | 115.1 | 353.5 | 222.2 |
| $5^{th}$ percentile | 55.3 | 50.6 | 33.5 | 27.0 | 15.1 | 10.5 | 3.7 | 2.7 |
| $25^{th}$ percentile | 82.5 | 74.9 | 66.0 | 51.8 | 42.1 | 28.6 | 15.4 | 11.0 |
| Median | 108.8 | 95.1 | 106.1 | 79.9 | 84.7 | 55.8 | 41.9 | 29.2 |
| $75^{th}$ percentile | 142.7 | 119.1 | 168.9 | 121.6 | 172.9 | 108.9 | 113.3 | 77.0 |
| $95^{th}$ percentile | 209.7 | 161.1 | 330.4 | 219.9 | 471.7 | 280.6 | 469.4 | 308.6 |
| Proportion (%) | 88.2 | 11.8 | 95.1 | 4.9 | 97.7 | 2.3 | 88.0 | 12.0 |
| **Panel B: Summary statistics of benefits for a death benefit parameter of 75%** | | | | | | | | |
| | 75 | | 85 | | 95 | | 105 | |
| | Dynamic | Static | Dynamic | Static | Dynamic | Static | Dynamic | Static |
| Average | 106.0 | 89.3 | 95.4 | 68.0 | 57.2 | 34.6 | 15.9 | 8.4 |
| Standard deviation | 44.3 | 30.8 | 74.6 | 46.3 | 82.3 | 44.4 | 48.8 | 23.5 |
| $5^{th}$ percentile | 49.9 | 45.7 | 23.8 | 19.1 | 5.7 | 4.0 | 0.4 | 0.2 |
| $25^{th}$ percentile | 74.3 | 67.5 | 46.8 | 36.7 | 16.1 | 10.8 | 1.7 | 1.0 |
| Median | 98.1 | 85.7 | 75.4 | 56.5 | 32.7 | 21.3 | 4.9 | 2.8 |
| $75^{th}$ percentile | 128.7 | 107.3 | 120.0 | 86.1 | 67.0 | 41.6 | 13.9 | 7.7 |
| $95^{th}$ percentile | 189.2 | 145.1 | 234.4 | 155.4 | 184.5 | 108.0 | 59.8 | 31.5 |
| Proportion (%) | 88.3 | 11.7 | 95.2 | 4.8 | 97.9 | 2.1 | 98.2 | 1.8 |

*Notes:* This table reports summary statistics of benefits in thousands of dollars for four ages of interest (75, 85, 95, and 105 years old) and for the two allocation strategies. We consider the basic setting of Section 5 as well as death benefit parameters of 25% (Panel A) and 75% (Panel B). The proportion value for the dynamic case reports the proportion of scenarios with a higher value of benefit for the dynamic strategy when compared to the static case. The proportion value for the static case is the opposite.

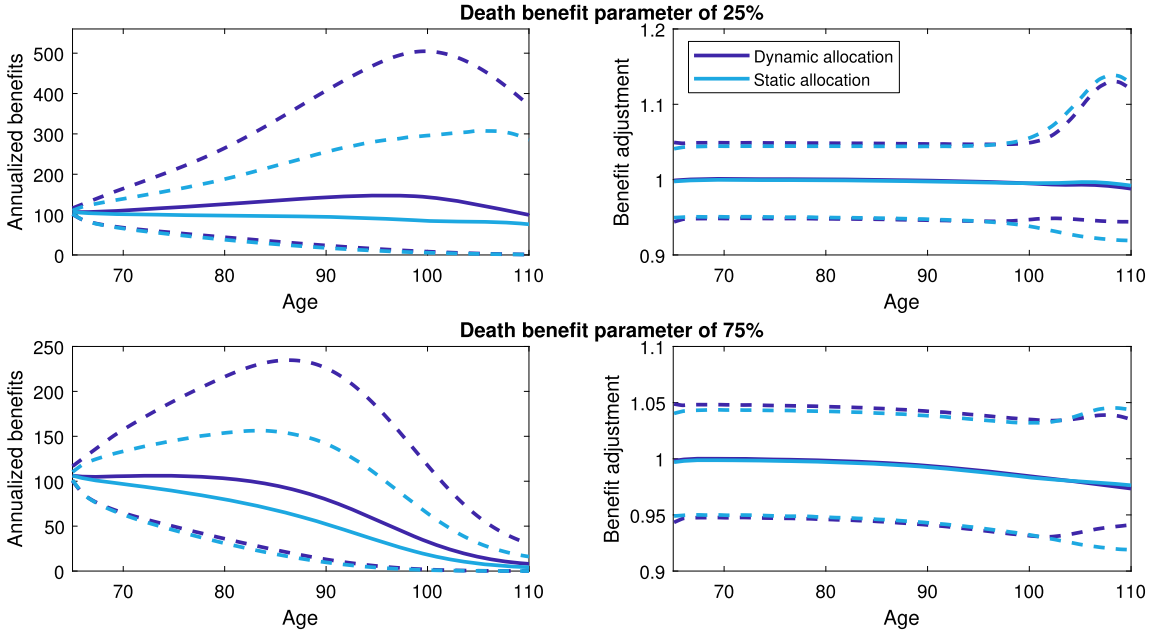


**Fig. 7. Annualized benefits and benefit adjustments funnels of doubt for dynamic and static asset allocations with death benefits**. *Notes:* This figure reports funnels of doubt for the annualized benefits in thousands of dollars and benefit adjustments. We consider dynamic and static allocation strategies along with the basic setting of Section 5 and two different death benefit parameters (25% and 75%). Average values (solid lines) as well as $5^{th}$ and $95^{th}$ percentiles (dashed lines) are reported.

Note that these additional returns, stemming from the heightened allocation to the risky asset, contribute significantly to the benefit streams. Yet they are oftentimes based on highly leveraged positions that might not be possible in real applications. Section 6.1 will comment on this issue.

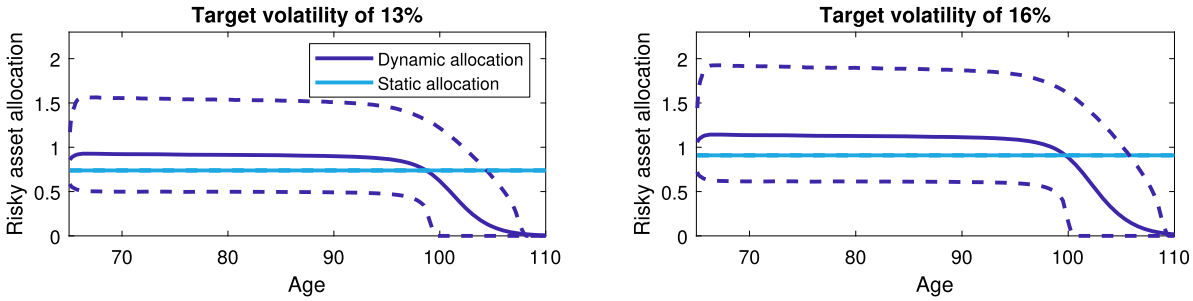


**Fig. 8. Risky asset allocation funnels of doubt for dynamic and static asset allocation with different volatility targets**. *Notes:* This figure shows funnels of doubt for the risky asset allocation $\omega_t$. We consider dynamic and static allocation along with the basic setting of Section 5 and two different volatility targets: 13% (left panel) and 16% (right panel). Average values (solid lines) as well as 5$^{th}$ and 95$^{th}$ percentiles (dashed lines) are reported. Note that the static allocation strategy is constant through time, hence leading to degenerate funnels.

**Table 4**
Summary statistics of benefits with different volatility targets.

| **Panel A: Summary statistics of benefits for a volatility target of 13%** | | | | | | | | |
|---|---|---|---|---|---|---|---|---|
| | 75 | | 85 | | 95 | | 105 | |
| | Dynamic | Static | Dynamic | Static | Dynamic | Static | Dynamic | Static |
| Average | 146.5 | 116.8 | 200.1 | 128.2 | 314.3 | 164.7 | 510.3 | 304.3 |
| Standard deviation | 78.8 | 50.4 | 193.9 | 103.0 | 545.6 | 241.3 | 1743.1 | 991.4 |
| 5$^{th}$ percentile | 54.9 | 48.9 | 36.4 | 27.6 | 22.4 | 14.3 | 10.4 | 6.8 |
| 25$^{th}$ percentile | 91.2 | 80.9 | 81.7 | 60.5 | 70.9 | 43.8 | 48.9 | 31.7 |
| Median | 129.3 | 109.4 | 143.4 | 100.4 | 156.8 | 92.4 | 143.1 | 90.2 |
| 75$^{th}$ percentile | 182.6 | 144.7 | 248.9 | 163.3 | 349.4 | 192.8 | 421.1 | 258.8 |
| 95$^{th}$ percentile | 295.6 | 209.9 | 552.5 | 321.5 | 1087.6 | 541.0 | 1953.6 | 1159.9 |
| Proportion (%) | 88.0 | 12.0 | 95.0 | 5.0 | 97.6 | 2.4 | 87.5 | 12.5 |
| **Panel B: Summary statistics of benefits for a volatility target of 16%** | | | | | | | | |
| | 75 | | 85 | | 95 | | 105 | |
| | Dynamic | Static | Dynamic | Static | Dynamic | Static | Dynamic | Static |
| Average | 172.6 | 129.6 | 250.7 | 142.7 | 420.2 | 184.1 | 735.3 | 342.5 |
| Standard deviation | 115.7 | 67.9 | 300.8 | 134.9 | 907.1 | 313.0 | 3025.3 | 1283.7 |
| 5$^{th}$ percentile | 50.5 | 43.7 | 32.0 | 22.7 | 19.4 | 11.2 | 9.2 | 5.2 |
| 25$^{th}$ percentile | 94.0 | 81.5 | 82.6 | 57.7 | 71.5 | 39.9 | 50.8 | 27.8 |
| Median | 143.6 | 117.3 | 159.7 | 103.9 | 175.1 | 91.8 | 163.5 | 86.5 |
| 75$^{th}$ percentile | 218.2 | 164.4 | 304.6 | 181.5 | 430.9 | 206.8 | 530.9 | 266.8 |
| 95$^{th}$ percentile | 390.0 | 256.6 | 768.3 | 392.5 | 1548.8 | 643.6 | 2797.6 | 1314.1 |
| Proportion (%) | 87.8 | 12.2 | 94.8 | 5.2 | 97.6 | 2.4 | 91.6 | 8.4 |

*Notes:* This table reports summary statistics of benefits in thousands of dollars for four ages of interest (75, 85, 95, and 105 years old) and for the two allocation strategies. We consider the basic setting of Section 5 and two different volatility targets: 13% (Panel A) and 16% (Panel B). The proportion value for the dynamic case reports the proportion of scenarios with a higher value of benefit for the dynamic strategy when compared to the static case. The proportion value for the static case is the opposite.

### *5.4. Pool sizes and impact on investment strategies*

As depicted in Fig. 2, the size of the pool can impact the risky asset allocation: a smaller pool increases the volatility stemming from mortality-related adjustments, consequently leading to a decrease in the allocation to the risky asset, generally speaking. We now assess the importance of this assumption.

Fig. 9 presents funnels of doubt for risky asset allocation distributions; the funnels are similar to those presented in Fig. 4, with one notable distinction: the decrease in the allocation is more pronounced for smaller pools. In particular, when dealing with pool sizes of 250 and 500 members at inception, the risky asset allocation diminishes to zero in all scenarios when members reach the ages of 100 and 103 years, respectively. This contrasts with the baseline case of Section 5.1, which involves 1,000 members, where the allocation reaches zero at the age of 107. The general decrease in the allocation is a by-product of the increased benefit adjustment volatility for small pools.

The benefits tend to be generally larger under the dynamic strategy and during the first 30 years; as in the baseline case, the dynamic allocation leads to benefits that are larger in about 90% of the scenarios (see Table 5 for more details). After this period, however, benefits can become lower when using the dynamic strategy due to the low allocation to the risky asset. For a pool of 500 members at inception, the outcomes still seem better for the dynamic strategy at these higher ages. For very small pools of 250 members at inception, however, the benefits are comparable for both strategies—neither better nor worse.[25] It is therefore recommended to be careful when setting up lifetime pension pools with so few members at the start.

[25] After 30 years, a pool with an initial size of 250 members has about 35 members left, which is a very low number in this context.

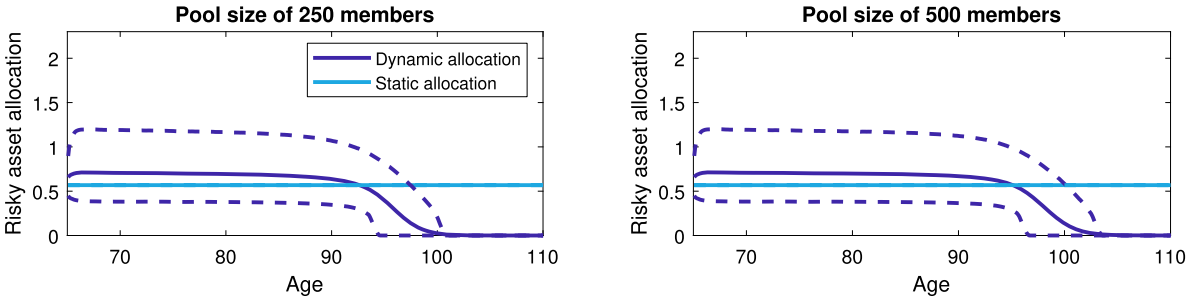


**Fig. 9. Risky asset allocation funnels of doubt for dynamic and static asset allocation and for different pool sizes at inception**. *Notes:* This figure shows funnels of doubt for the risky asset allocation $\omega_t$. We consider dynamic and static allocation along with the basic setting of Section 5 and two different pool sizes at inception: 250 members (left panel) and 500 members (right panel). Average values (solid lines) as well as 5$^{th}$ and 95$^{th}$ percentiles (dashed lines) are reported. Note that the static allocation strategy is constant through time, hence leading to degenerate funnels.

**Table 5**
Summary statistics of benefits for pool sizes of 250 and 500 members at inception.

| **Panel A: Summary statistics of benefits for a pool size of 250 members at inception** | | | | | | | | |
|---|---|---|---|---|---|---|---|---|
| | 75 | | 85 | | 95 | | 105 | |
| | Dynamic | Static | Dynamic | Static | Dynamic | Static | Dynamic | Static |
| Average | 123.4 | 104.4 | 158.4 | 114.8 | 223.7 | 150.9 | 263.9 | 262.0 |
| Standard deviation | 51.5 | 36.2 | 123.6 | 78.8 | 311.1 | 194.6 | 797.9 | 764.2 |
| 5$^{th}$ percentile | 58.2 | 53.3 | 39.5 | 31.9 | 23.2 | 16.9 | 7.2 | 7.1 |
| 25$^{th}$ percentile | 86.7 | 78.8 | 77.9 | 61.6 | 64.3 | 46.6 | 30.7 | 30.6 |
| Median | 114.2 | 100.2 | 125.1 | 95.3 | 130.1 | 91.9 | 85.1 | 84.7 |
| 75$^{th}$ percentile | 149.9 | 125.4 | 199.0 | 145.1 | 264.5 | 181.2 | 233.7 | 232.3 |
| 95$^{th}$ percentile | 220.2 | 170.0 | 388.5 | 263.2 | 716.8 | 471.4 | 997.6 | 992.4 |
| Proportion (%) | 88.0 | 12.0 | 94.7 | 5.3 | 95.0 | 5.0 | 49.1 | 50.9 |
| **Panel B: Summary statistics of benefits for a pool size of 500 members at inception** | | | | | | | | |
| | 75 | | 85 | | 95 | | 105 | |
| | Dynamic | Static | Dynamic | Static | Dynamic | Static | Dynamic | Static |
| Average | 123.5 | 104.3 | 159.2 | 114.6 | 232.6 | 148.4 | 329.2 | 283.0 |
| Standard deviation | 51.6 | 36.1 | 124.3 | 78.4 | 327.4 | 190.2 | 1006.6 | 889.9 |
| 5$^{th}$ percentile | 58.2 | 53.3 | 39.7 | 32.0 | 23.8 | 16.9 | 9.3 | 8.1 |
| 25$^{th}$ percentile | 86.7 | 78.8 | 78.3 | 61.5 | 66.7 | 46.4 | 39.1 | 34.0 |
| Median | 114.3 | 100.1 | 125.7 | 95.2 | 133.8 | 90.6 | 107.1 | 92.8 |
| 75$^{th}$ percentile | 150.1 | 125.4 | 200.2 | 145.0 | 273.7 | 178.1 | 291.0 | 251.6 |
| 95$^{th}$ percentile | 220.4 | 169.7 | 391.1 | 262.6 | 746.5 | 464.5 | 1241.9 | 1071.2 |
| Proportion (%) | 88.1 | 11.9 | 94.9 | 5.1 | 97.1 | 2.9 | 65.5 | 34.5 |

*Notes:* This table reports summary statistics of benefits in thousands of dollars for four ages of interest (75, 85, 95, and 105 years old) and for the two allocation strategies. We consider the basic setting of Section 5 and two initial pool sizes: 250 members (Panel A) and 500 members (Panel B). The proportion value for the dynamic case reports the proportion of scenarios with a higher value of benefit for the dynamic strategy when compared to the static case. The proportion value for the static case is the opposite.

## 6. Limitations in practical situations

This section investigates and assesses the impact of three practical limitations of the dynamic volatility-targeting allocation introduced above: leverage constraints, brokerage fees, and rebalancing frequencies.

### *6.1. Leverage constraints*

Leverage refers to the use of borrowed capital by financial institutions and investors to enhance their returns. As evidenced by Fig. 4, we know that such leverage is used in the dynamic strategy as the risky asset allocation is sometimes above one (e.g., the 95$^{th}$ percentile of the risky asset allocation distribution is above one for ages 65 to 98).

In practice, certain pool operators may face restrictions on the amount of borrowed capital they can employ: some might have *soft* restrictions (i.e., allowed to use some leverage) or *strict* restrictions (i.e., no leverage whatsoever). Accordingly, we investigate the impact of having a cap on the allocation to the risky asset as it might impact our results in a non-trivial way. Specifically, in this study, we modify the weight of Equation (20) by taking the minimum of the computed allocation and the limit.

We explore the effects of two distinct limits imposed on risky asset allocations: 100% and 150%. New risky asset allocation funnels of doubt for these two limits are presented in Fig. 10: the left panel reports the results for a limit of 100% and the right panel for a limit of 150%. Applying this limit impacts the right tail of the risky asset allocation distribution; for instance, when the limit is set to 100%, we observe a narrower funnel of doubt driven by the 95$^{th}$ percentile being lower than that of Fig. 4. When the limit is 150%, on the other hand, we only see minimal changes in the allocations as less than 1% of the optimal weights were above 1.5 in the baseline case.

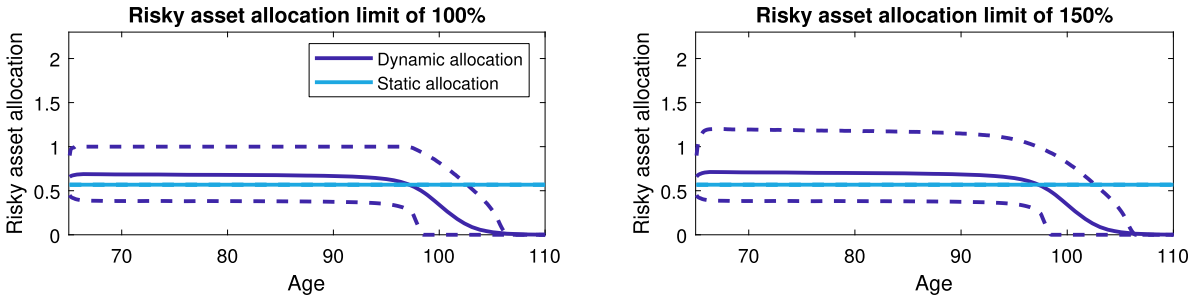


**Fig. 10. Risky asset allocation funnels of doubt for dynamic and static asset allocation and with leverage constraints**. *Notes:* This figure shows funnels of doubt for the risky asset allocation $\omega_t$. We consider dynamic and static allocation along with the basic setting of Section 5 and two different leverage limit levels: 100% (left panel) and 150% (right panel). Average values (solid lines) as well as 5$^{\text{th}}$ and 95$^{\text{th}}$ percentiles (dashed lines) are reported. Note that the static allocation strategy is constant through time, hence leading to degenerate funnels.

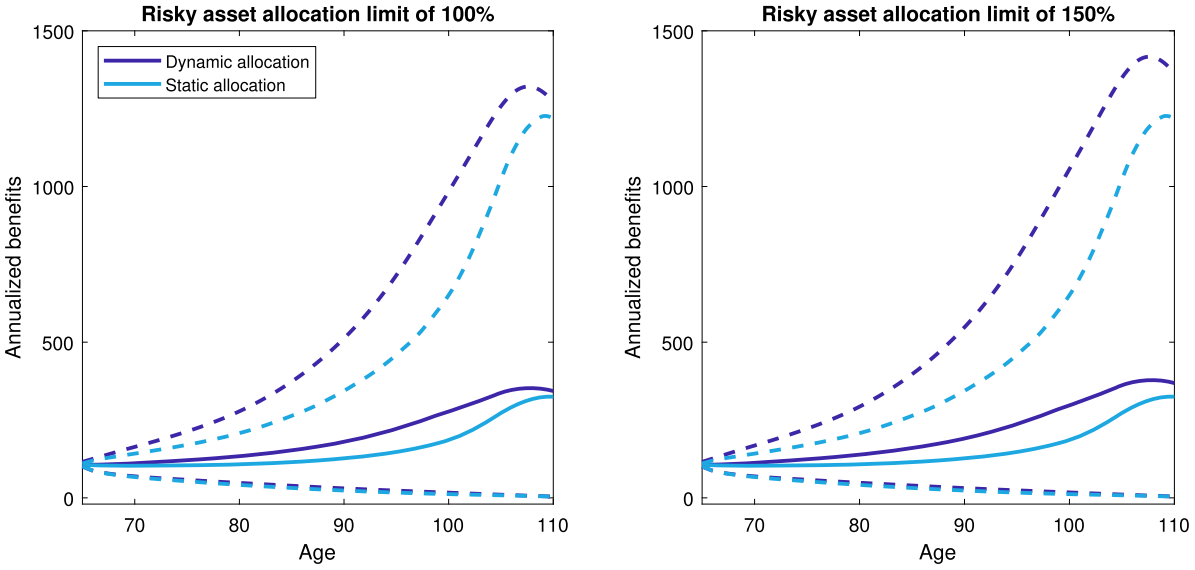


**Fig. 11. Annualized benefits funnels of doubt for dynamic and static asset allocations and with leverage constraints**. *Notes:* This figure reports funnels of doubt for the annualized benefits. We consider dynamic and static allocation strategies along with the basic setting of Section 5 and two different leverage constraint levels: 100% (top panels) and 150% (bottom panels). Average values (solid lines) as well as 5$^{\text{th}}$ and 95$^{\text{th}}$ percentiles (dashed lines) are reported.

Fig. 11 provides insight into the annualized benefits; for a leverage limit level of 100%, the annualized benefits appear slightly lower when compared to those presented in Fig. 5. The dynamic asset allocation strategy leads, nonetheless, to higher benefits in most cases. Conversely, when the limit is 150% (right panels), the funnels of doubt closely resemble those presented in Fig. 5, reaffirming that most allocations were already below 150% in the baseline case.

The results of Fig. 11 are further supported by Table 6: a limit of 100% marginally impacts the superiority of the dynamic strategy, whereas a limit of 150% does not impact the results from the baseline case of Section 5.

### 6.2. Brokerage fees

Brokerage fees represent charges or commissions levied by financial intermediaries for facilitating the execution of securities transactions on behalf of investors. Brokerage fees, while a standard aspect of investment transactions, can influence an investor's overall returns and should be carefully considered when formulating investment strategies. For instance, in the context of the volatility-targeting strategy, such commissions and fees could negatively impact the benefits if the allocation were to change too often.

The specific fee structure and rates associated with brokerage services can vary significantly across different brokerage firms and jurisdictions. This study relies on a very simple fee structure that is proportional to the size of the transaction. Let $\upsilon$ be the brokerage fee. The time-$t$ broker fee's dollar amount is therefore given by

$$\upsilon \times \left| \left(F_{t-h} - B_{t-h}\right) \omega_t \frac{S_t}{S_{t-h}} - \left(F_t - B_t\right) \omega_{t+h} \right|,$$

which captures the (absolute value of the) difference between the end of period amount invested in the risky asset and the new dollar amount position after benefit distribution. Note that we apply these fees to both dynamic and static strategies.[26]

[26] Even with a static strategy, the pool operator needs to rebalance to keep the allocation holdings *static*.

**Table 6**
Summary statistics of benefits with leverage constraints.

| **Panel A: Summary statistics of benefits with a risky asset allocation limit of 100%** | | | | | | | | |
|---|---|---|---|---|---|---|---|---|
| | 75 | | 85 | | 95 | | 105 | |
| | Dynamic | Static | Dynamic | Static | Dynamic | Static | Dynamic | Static |
| Average | 120.7 | 104.4 | 151.9 | 114.4 | 220.4 | 146.7 | 335.4 | 269.9 |
| Standard deviation | 48.6 | 36.1 | 115.8 | 78.2 | 307.2 | 187.9 | 964.8 | 775.5 |
| $5^{th}$ percentile | 58.0 | 53.3 | 39.0 | 32.0 | 23.3 | 17.1 | 10.2 | 8.3 |
| $25^{th}$ percentile | 85.9 | 78.9 | 76.0 | 61.5 | 64.3 | 46.1 | 42.1 | 34.3 |
| Median | 112.4 | 100.2 | 121.1 | 95.0 | 128.7 | 90.3 | 113.2 | 91.5 |
| $75^{th}$ percentile | 146.3 | 125.5 | 191.4 | 144.7 | 260.6 | 176.5 | 303.2 | 245.0 |
| $95^{th}$ percentile | 211.8 | 169.8 | 368.5 | 261.4 | 705.6 | 454.8 | 1271.3 | 1015.8 |
| Proportion (%) | 87.7 | 12.3 | 94.6 | 5.4 | 97.2 | 2.8 | 75.6 | 24.4 |
| **Panel B: Summary statistics of benefits with a risky asset allocation limit of 150%** | | | | | | | | |
| | 75 | | 85 | | 95 | | 105 | |
| | Dynamic | Static | Dynamic | Static | Dynamic | Static | Dynamic | Static |
| Average | 123.6 | 104.4 | 159.3 | 114.4 | 235.5 | 146.7 | 359.4 | 269.9 |
| Standard deviation | 51.6 | 36.1 | 124.5 | 78.2 | 334.9 | 187.9 | 1045.4 | 775.5 |
| $5^{th}$ percentile | 58.3 | 53.3 | 39.7 | 32.0 | 24.2 | 17.1 | 10.6 | 8.3 |
| $25^{th}$ percentile | 86.8 | 78.9 | 78.3 | 61.5 | 67.2 | 46.1 | 44.4 | 34.3 |
| Median | 114.5 | 100.2 | 125.8 | 95.0 | 135.6 | 90.3 | 119.8 | 91.5 |
| $75^{th}$ percentile | 150.2 | 125.5 | 200.1 | 144.7 | 277.2 | 176.5 | 323.6 | 245.0 |
| $95^{th}$ percentile | 220.6 | 169.8 | 392.1 | 261.4 | 757.4 | 454.8 | 1363.2 | 1015.8 |
| Proportion (%) | 88.2 | 11.8 | 95.0 | 5.0 | 97.5 | 2.5 | 79.6 | 20.4 |

*Notes:* This table reports summary statistics of benefits in thousands of dollars for four ages of interest (75, 85, 95, and 105 years old) and for the two allocation strategies. We consider the basic setting of Section 5 and leverage limit levels of 100% (Panel A) and 150% (Panel B). The proportion value for the dynamic case reports the proportion of scenarios with a higher value of benefit for the dynamic strategy when compared to the static case. The proportion value for the static case is the opposite.

This study considers two different broker fee levels: 10 basis points (bps) and 50 bps. The first case is inspired from the results of Di Maggio et al. (2022) who found the average broker fee to be roughly 13 bps relative to the value of transactions. The second is an extreme case, allowing us to quantify the impact of very high broker fees.

The left panel of Fig. 12 and Panel A of Table 7 provide insights into the annualized benefits when the broker fee is set to 10 bps. The impact of such a brokerage fee on the static strategy is relatively modest overall. In contrast, its impact on the dynamic strategy is more noticeable, resulting in a funnel of doubt that is slightly lower than that of Fig. 5, with reduction in the annualized benefits between $3,000 and $15,000, on average. Yet the dynamic strategy still yields significantly higher benefits when compared to the static allocation approach, and this for the majority of the scenarios.

When the broker fee is increased to 50 bps (right panel of Fig. 12 and Panel B of Table 7), the effects of the commission become more pronounced, leading to reductions in annualized benefits. For the first 35 years, the dynamic strategy still continues to deliver higher average benefits than the static strategy even with very high broker fees, but this trend reverses for members older than 100 years old. This is also true for most percentiles in Table 7.

It is worth emphasizing that a 10 bps broker fee aligns more closely with empirical observations (see, e.g., Di Maggio et al., 2022), and that 50 bps—an extreme fee—would still see benefit improvements for most of the members' lifetime. However, one should be careful as high brokerage fees can definitely impact the viability and success of lifetime pension pools.

### *6.3. Rebalancing frequency*

The last practical concern we investigate in this study is the rebalancing frequency—the frequency at which an investment portfolio is adjusted. To simplify the presentation and our calculations, we also consistently change the frequency at which the benefits are paid to preserve the consistency between the volatility target of Equation (19) and the allocation of Equation (20).[27] Specifically, in addition to the monthly case considered above, we consider five values of $m$ in this analysis: 1 (annual frequency), 2 (semiannual frequency), 6 (bimonthly frequency), 26 (biweekly frequency), and 52 (weekly frequency).

Table 8 presents a summary of various statistics for the five additional values of $m$. Notably, the average benefits are systematically higher for all ages and frequencies under consideration. However, at the annual frequency, and particularly as the pool approaches termination, certain percentiles of the benefit distribution are lower when employing the dynamic strategy. Nonetheless, the dynamic allocation strategy continues to deliver robust benefits until members approach 100 years of age. For all other frequencies higher than annual, the benefit streams consistently demonstrate superior performance when employing the dynamic strategy. The proportion of paths resulting in higher benefits is overall greater when utilizing the dynamic allocation method.

The effectiveness of the dynamic strategy appears to be closely tied to the rebalancing frequency, with significant improvements as the frequency increases. The average (annualized) benefit across the entire period exhibits a clear upward trend in relation to the rebalancing frequency,

[27] It would be possible to decouple these two operations, but this is more involved. We leave this interesting question for future research.

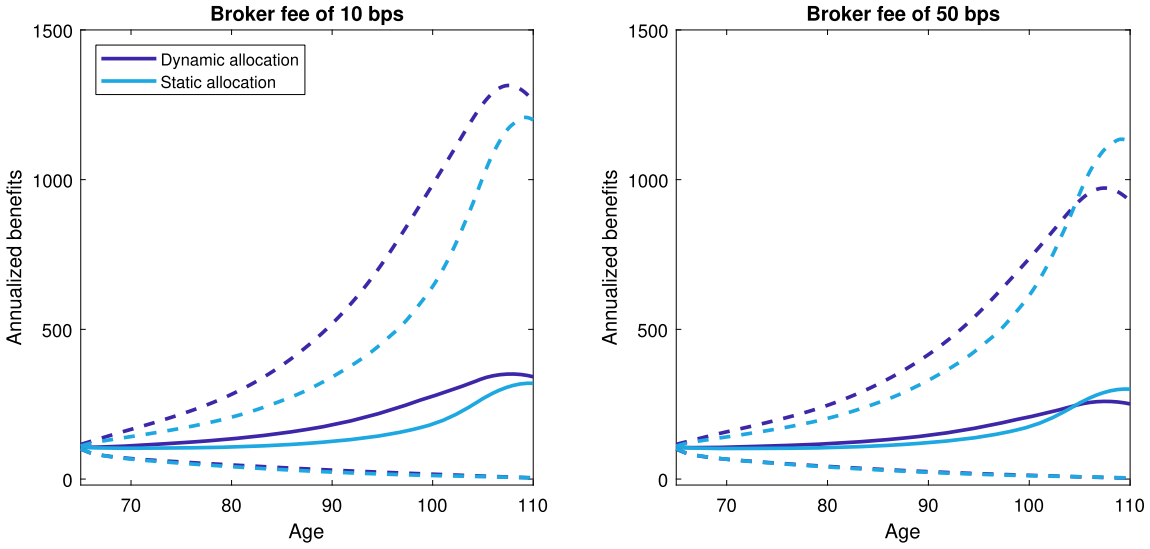


**Fig. 12. Annualized benefits funnels of doubt for dynamic and static asset allocations and with brokerage fees**. *Notes:* This figure reports funnels of doubt for the annualized benefits. We consider dynamic and static allocation strategies along with the basic setting of Section 5 and two different commission levels: 10 basis points (left panel) and 50 basis points (right panel). Average values (solid lines) as well as 5$^{th}$ and 95$^{th}$ percentiles (dashed lines) are reported.

**Table 7**
Summary statistics of benefits with brokerage fees.

| **Panel A: Summary statistics of benefits with a broker fee of 10 bps** | | | | | | | | |
|---|---|---|---|---|---|---|---|---|
| | 75 | | 85 | | 95 | | 105 | |
| | Dynamic | Static | Dynamic | Static | Dynamic | Static | Dynamic | Static |
| Average | 121.0 | 104.0 | 152.8 | 113.6 | 221.2 | 145.3 | 334.0 | 266.1 |
| Standard deviation | 50.3 | 35.9 | 119.0 | 77.7 | 313.7 | 186.0 | 969.0 | 765.0 |
| 5$^{th}$ percentile | 57.3 | 53.1 | 38.3 | 31.7 | 22.9 | 16.9 | 9.9 | 8.2 |
| 25$^{th}$ percentile | 85.1 | 78.6 | 75.3 | 61.1 | 63.4 | 45.6 | 41.4 | 33.8 |
| Median | 112.1 | 99.9 | 120.7 | 94.4 | 127.6 | 89.4 | 111.5 | 90.3 |
| 75$^{th}$ percentile | 147.0 | 125.0 | 191.9 | 143.7 | 260.5 | 174.7 | 300.8 | 241.6 |
| 95$^{th}$ percentile | 215.7 | 169.2 | 375.2 | 259.8 | 710.9 | 450.3 | 1265.1 | 1001.6 |
| Proportion (%) | 85.3 | 14.7 | 92.8 | 7.2 | 95.8 | 4.2 | 74.5 | 25.5 |
| **Panel B: Summary statistics of benefits with a broker fee of 50 bps** | | | | | | | | |
| | 75 | | 85 | | 95 | | 105 | |
| | Dynamic | Static | Dynamic | Static | Dynamic | Static | Dynamic | Static |
| Average | 111.0 | 102.5 | 128.7 | 110.6 | 171.6 | 139.5 | 248.1 | 251.7 |
| Standard deviation | 45.3 | 35.5 | 99.0 | 75.7 | 240.8 | 178.8 | 713.8 | 724.1 |
| 5$^{th}$ percentile | 53.4 | 52.2 | 32.9 | 30.8 | 18.1 | 16.2 | 7.5 | 7.7 |
| 25$^{th}$ percentile | 78.7 | 77.4 | 64.2 | 59.4 | 49.8 | 43.8 | 31.1 | 31.9 |
| Median | 103.0 | 98.4 | 102.2 | 91.8 | 99.7 | 85.8 | 83.5 | 85.3 |
| 75$^{th}$ percentile | 134.5 | 123.3 | 161.8 | 139.9 | 202.5 | 167.7 | 224.3 | 228.5 |
| 95$^{th}$ percentile | 196.3 | 166.9 | 313.4 | 253.1 | 549.8 | 432.5 | 939.9 | 947.7 |
| Proportion (%) | 68.4 | 31.6 | 74.9 | 25.1 | 77.7 | 22.3 | 46.9 | 53.1 |

*Notes:* This table reports summary statistics of benefits in thousands of dollars for four ages of interest (75, 85, 95, and 105 years old) and for the two allocation strategies. We consider the basic setting of Section 5 and two different commission levels: 10 basis points (Panel A) and 50 basis points (Panel B). The proportion value for the dynamic case reports the proportion of scenarios with a higher value of benefit for the dynamic strategy when compared to the static case. The proportion value for the static case is the opposite.

starting at $152,900 for an annual frequency and rising to $372,100 for a weekly frequency. Examining the results for biweekly and weekly frequencies (Panels D and E of Table 8, respectively), these higher frequencies yield larger benefits throughout the period of interest. In fact, the dynamic strategy consistently outperforms static allocations in over 90% of the scenarios, underscoring the advantages of more frequent rebalancing. The difference is very significant for advanced ages, where rebalancing more frequently improves the benefit streams. Hence, it might be in the pool operator's best interest to rebalance the portfolio often to ensure that the allocation is consistent with the current volatility conditions.

Adjusting the asset allocation frequently can incur costs, however. The concern with such frequent changes lies in the potential for additional brokerage expenses to offset the benefits gained from the increased rebalancing frequency. To gauge the broker fee's impact in the context of frequent rebalancing—at a weekly frequency for instance—we revisit the scenario outlined in Section 6.2 with $m = 52$ and $\upsilon = 10$ bps. The resulting

**Table 8**
Summary statistics of benefits for different rebalancing frequencies.

| **Panel A: Summary statistics of benefits for an annual frequency** | | | | | | | | |
|---|---|---|---|---|---|---|---|---|
| | 75 | | 85 | | 95 | | 105 | |
| | Dynamic | Static | Dynamic | Static | Dynamic | Static | Dynamic | Static |
| Average | 108.2 | 99.9 | 125.6 | 109.3 | 164.1 | 139.2 | 226.7 | 244.9 |
| Standard deviation | 42.0 | 32.8 | 89.6 | 71.6 | 204.0 | 169.6 | 541.0 | 663.4 |
| $5^{th}$ percentile | 52.3 | 53.3 | 33.5 | 32.3 | 19.3 | 17.5 | 8.8 | 8.7 |
| $25^{th}$ percentile | 78.1 | 76.7 | 65.2 | 60.5 | 52.3 | 45.9 | 34.3 | 34.2 |
| Median | 101.8 | 96.2 | 102.5 | 91.9 | 101.9 | 88.0 | 87.2 | 88.2 |
| $75^{th}$ percentile | 131.0 | 119.1 | 159.1 | 137.9 | 199.5 | 168.7 | 222.3 | 231.0 |
| $95^{th}$ percentile | 185.9 | 159.2 | 295.5 | 245.1 | 506.2 | 423.7 | 837.1 | 908.4 |
| Proportion (%) | 77.1 | 22.9 | 82.3 | 17.7 | 83.5 | 16.5 | 47.9 | 52.1 |
| **Panel B: Summary statistics of benefits for a semiannual frequency** | | | | | | | | |
| | 75 | | 85 | | 95 | | 105 | |
| | Dynamic | Static | Dynamic | Static | Dynamic | Static | Dynamic | Static |
| Average | 113.0 | 102.3 | 134.8 | 112.2 | 182.0 | 143.3 | 260.0 | 256.6 |
| Standard deviation | 46.1 | 34.6 | 101.5 | 75.1 | 243.2 | 178.6 | 721.3 | 730.2 |
| $5^{th}$ percentile | 53.3 | 53.4 | 34.4 | 32.2 | 19.8 | 17.3 | 8.7 | 8.3 |
| $25^{th}$ percentile | 80.0 | 77.8 | 67.7 | 61.2 | 54.5 | 46.1 | 35.2 | 34.2 |
| Median | 105.4 | 98.4 | 107.9 | 93.8 | 108.4 | 89.4 | 92.2 | 89.4 |
| $75^{th}$ percentile | 137.3 | 122.4 | 170.2 | 141.8 | 217.1 | 173.0 | 244.0 | 237.4 |
| $95^{th}$ percentile | 198.9 | 164.9 | 326.3 | 254.8 | 574.9 | 442.0 | 966.5 | 957.9 |
| Proportion (%) | 78.6 | 21.4 | 85.5 | 14.5 | 88.3 | 11.7 | 54.4 | 45.6 |
| **Panel C: Summary statistics of benefits for a bimonthly frequency** | | | | | | | | |
| | 75 | | 85 | | 95 | | 105 | |
| | Dynamic | Static | Dynamic | Static | Dynamic | Static | Dynamic | Static |
| Average | 118.7 | 103.9 | 147.2 | 114.0 | 209.2 | 146.5 | 316.5 | 272.8 |
| Standard deviation | 49.6 | 35.7 | 114.6 | 77.6 | 293.1 | 186.2 | 882.5 | 757.1 |
| $5^{th}$ percentile | 55.4 | 53.3 | 36.6 | 32.0 | 21.6 | 17.1 | 9.5 | 8.3 |
| $25^{th}$ percentile | 83.3 | 78.7 | 72.4 | 61.5 | 60.2 | 46.3 | 39.5 | 34.8 |
| Median | 109.9 | 99.8 | 116.2 | 94.8 | 121.2 | 90.4 | 106.5 | 92.7 |
| $75^{th}$ percentile | 144.3 | 124.8 | 185.1 | 144.1 | 246.3 | 176.4 | 284.4 | 246.4 |
| $95^{th}$ percentile | 211.7 | 168.8 | 362.0 | 261.3 | 670.4 | 453.9 | 1185.9 | 1010.8 |
| Proportion (%) | 82.3 | 17.7 | 90.2 | 9.8 | 93.6 | 6.4 | 67.2 | 32.8 |
| **Panel D: Summary statistics of benefits for a biweekly frequency** | | | | | | | | |
| | 75 | | 85 | | 95 | | 105 | |
| | Dynamic | Static | Dynamic | Static | Dynamic | Static | Dynamic | Static |
| Average | 134.3 | 104.5 | 187.9 | 114.3 | 303.6 | 147.7 | 484.2 | 271.9 |
| Standard deviation | 56.1 | 36.2 | 147.9 | 78.2 | 433.0 | 189.6 | 1339.6 | 743.3 |
| $5^{th}$ percentile | 63.1 | 53.2 | 46.0 | 31.5 | 30.5 | 16.8 | 14.1 | 8.3 |
| $25^{th}$ percentile | 94.5 | 79.0 | 92.0 | 61.4 | 85.5 | 46.2 | 59.4 | 34.7 |
| Median | 124.1 | 100.2 | 147.6 | 94.9 | 174.6 | 91.0 | 161.2 | 93.1 |
| $75^{th}$ percentile | 163.1 | 125.3 | 236.2 | 144.8 | 355.5 | 177.5 | 436.0 | 249.9 |
| $95^{th}$ percentile | 239.9 | 170.6 | 464.8 | 261.7 | 986.9 | 460.2 | 1827.5 | 1029.5 |
| Proportion (%) | 96.4 | 3.6 | 99.4 | 0.6 | 99.8 | 0.2 | 94.4 | 5.6 |
| **Panel E: Summary statistics of benefits for a weekly frequency** | | | | | | | | |
| | 75 | | 85 | | 95 | | 105 | |
| | Dynamic | Static | Dynamic | Static | Dynamic | Static | Dynamic | Static |
| Average | 153.3 | 104.6 | 243.5 | 114.7 | 442.4 | 148.0 | 747.9 | 273.0 |
| Standard deviation | 63.6 | 36.3 | 190.7 | 78.6 | 626.8 | 191.1 | 2041.1 | 755.7 |
| $5^{th}$ percentile | 72.0 | 53.2 | 59.6 | 31.5 | 44.3 | 16.9 | 21.6 | 8.2 |
| $25^{th}$ percentile | 108.2 | 79.0 | 119.4 | 61.6 | 124.3 | 46.2 | 91.8 | 34.8 |
| Median | 141.9 | 100.4 | 191.7 | 95.1 | 253.9 | 91.2 | 247.8 | 93.3 |
| $75^{th}$ percentile | 185.9 | 125.5 | 306.7 | 145.3 | 518.9 | 177.7 | 678.8 | 249.5 |
| $95^{th}$ percentile | 273.1 | 170.8 | 602.3 | 263.0 | 1443.1 | 462.1 | 2872.3 | 1037.3 |
| Proportion (%) | 99.8 | 0.2 | 100.0 | 0.0 | 100.0 | 0.0 | 99.7 | 0.3 |

*Notes:* This table reports summary statistics of benefits in thousands of dollars for four ages of interest (75, 85, 95, and 105 years old) and for the two allocation strategies. We consider the basic setting of Section 5 and five different rebalancing frequencies: annual (Panel A), semiannual (Panel B), bimonthly (Panel C), biweekly (Panel D), and weekly (Panel E). The proportion value for the dynamic case reports the proportion of scenarios with a higher value of benefit for the dynamic strategy when compared to the static case. The proportion value for the static case is the opposite.

outcomes are detailed in Table SM.8 of the Supplementary Material: incorporating realistic broker fees does lead to a slight reduction in the benefit streams compared to those presented in Table 8. However, these benefits remain significantly higher than those achieved through the static strategy, and this holds true throughout the entire period of interest.

## 7. Concluding remarks

Previous research on lifetime pension pools primarily focused on basic investment strategies, such as constant allocations and strategies based solely on risk-free assets. However, recent studies proposed volatility-targeting strategies to enhance risk-adjusted returns and mitigate downside risk. These strategies have demonstrated the potential to improve investment performance (see, e.g., Olivieri et al., 2022; Li et al., 2022). They, however, considered investment risk only, neglecting the mortality risk that can become pronounced as pool members age.

This study addressed this gap by introducing a dynamic volatility-targeting strategy that simultaneously considers investment and mortality risks. We derived a strategy under realistic assumptions and assessed its performance through some analyses. Our findings indicate that the dynamic volatility-targeting approach yields more steady benefit streams, effectively reducing benefit risk by adjusting risky asset allocations during periods of heightened volatility.

Furthermore, our study explored the applicability of this strategy under various conditions, including cases with death benefits, smaller pool sizes, and different volatility targets. We also considered practical limitations related to leverage constraints, brokerage fees, and rebalancing frequencies. Our results demonstrated the strategy's robustness to these variations.

This study presented an approach to mitigate benefit risk over a lifetime pension pool's lifecycle. Yet, towards the end, the pool will contain only a handful of members—regardless of the allocation strategy used—and additional risk management techniques could be used by pool operators to further stabilize benefits in later years. Indeed, the question of what actions should be taken by operators when terminating pools is interesting and left for future research.

Another exciting question in our context relates to the impact of the mortality model on the end results. Various authors have shown that trend risk (Zhu and Bauer, 2022), prior ignorance (Girosi and King, 2008), and long memory (Peters et al., 2021) could have an impact on forecasting over longer horizons. Appendix A provides some additional analyses in which a different mortality improvement structure is assumed—long-memory dynamics for period effects. Investigating the impact of other modelling features is left for future work.

Finally, our study only considered one risky asset in the definition of the targeting strategy; this dynamic allocation methodology could be extended to cases where multiple classes of risky assets are considered. This future direction constitutes an interesting extension of our framework.

## CRediT authorship contribution statement

**Jean-François Bégin:** Writing – review & editing, Writing – original draft, Visualization, Validation, Software, Resources, Project administration, Methodology, Investigation, Funding acquisition, Formal analysis, Data curation, Conceptualization. **Barbara Sanders:** Writing – review & editing, Validation, Conceptualization.

## Declaration of competing interest

The authors declare that they have no known competing financial interests or personal relationships that could have appeared to influence the work reported in this paper.

## Data availability

The authors do not have permission to share data.

## Appendix A. Long memory in mortality improvements

Peters et al. (2021) demonstrate strong evidence for the existence of long memory features in mortality data. To verify if this could significantly impact our results, we replace the dynamics of $\kappa_1$ and $\kappa_2$ in Equations (10) and (11) with dynamics that allow for long memory. Specifically, we rely on an autoregressive fractionally integrated moving average (ARFIMA) model in the spirit of Zhou and Li (2023). This discrete-time model is based on annual observations; we further assume a constant force of mortality for fractional ages to obtain survival probabilities between integer ages (see Chapter 3.6 of Bowers et al., 1997, for more details).[28]

Table 9 mirrors Table 2 and provides summary statistics for the benefits (Panel A) and the benefit adjustments (Panel B) for the long-memory variant. Even though the numbers in the table are quantitatively different than those presented in Section 5, the results are qualitatively similar—the dynamic allocation strategy performs uniformly better than the static allocation. Two reasons can explain the differences between the results shown in Tables 2 and 9. First, the short-memory dynamics of Equations (10) and (11) tend to underestimate the variation in the future survival probabilities, whereas the long-memory model captures more of this dimension of uncertainty. Second, the short-memory dynamics lead to better improvements in the period effects that than those obtained with the long-memory model.

Despite these differences in the future mortality scenarios, the actual impact on the results of Table 9 is minimal, and the volatility targeting methodology proposed in this article is robust to this mortality assumption change. Indeed, we see similar trends to those of Table 2 and infer similar conclusions.

[28] Section SM.H of the Supplementary Material provides additional details on the long-memory model and the estimated parameters.

**Table 9**
Summary statistics of benefits and benefit adjustments for the long-memory mortality model.

| **Panel A: Summary statistics of benefits for the long-memory mortality model** | | | | | | | | |
|---|---|---|---|---|---|---|---|---|
| | 75 | | 85 | | 95 | | 105 | |
| | Dynamic | Static | Dynamic | Static | Dynamic | Static | Dynamic | Static |
| Average | 124.8 | 105.4 | 157.8 | 113.4 | 228.9 | 144.3 | 291.8 | 251.3 |
| Standard deviation | 51.8 | 36.4 | 122.1 | 76.9 | 316.7 | 182.2 | 920.6 | 735.4 |
| $5^{th}$ percentile | 58.4 | 53.3 | 39.6 | 31.6 | 23.2 | 16.4 | 7.6 | 6.8 |
| $25^{th}$ percentile | 87.9 | 80.0 | 77.6 | 60.8 | 65.0 | 44.8 | 32.7 | 29.0 |
| Median | 115.8 | 101.3 | 124.6 | 94.1 | 132.4 | 88.6 | 92.0 | 80.9 |
| $75^{th}$ percentile | 151.7 | 126.4 | 199.2 | 144.0 | 270.5 | 174.6 | 255.9 | 223.0 |
| $95^{th}$ percentile | 221.6 | 171.2 | 389.3 | 260.2 | 742.8 | 451.6 | 1117.2 | 965.2 |
| Proportion (%) | 88.1 | 11.9 | 95.1 | 4.9 | 97.2 | 2.8 | 64.0 | 36.0 |
| **Panel B: Summary statistics of benefit adjustments for the long-memory mortality model** | | | | | | | | |
| | 75 | | 85 | | 95 | | 105 | |
| | Dynamic | Static | Dynamic | Static | Dynamic | Static | Dynamic | Static |
| Average | 1.001 | 1.000 | 1.000 | 0.999 | 1.000 | 1.000 | 1.005 | 1.010 |
| Standard deviation | 0.109 | 0.103 | 0.117 | 0.112 | 0.139 | 0.144 | 0.547 | 0.559 |
| $5^{th}$ percentile | 0.948 | 0.950 | 0.944 | 0.945 | 0.935 | 0.933 | 0.905 | 0.894 |
| $25^{th}$ percentile | 0.982 | 0.983 | 0.979 | 0.980 | 0.973 | 0.972 | 0.941 | 0.940 |
| Median | 1.002 | 1.001 | 1.001 | 0.999 | 1.000 | 0.999 | 0.968 | 0.974 |
| $75^{th}$ percentile | 1.022 | 1.017 | 1.022 | 1.019 | 1.027 | 1.027 | 1.001 | 1.014 |
| $95^{th}$ percentile | 1.050 | 1.046 | 1.054 | 1.050 | 1.066 | 1.068 | 1.261 | 1.271 |
| Proportion (%) | 56.2 | 43.8 | 56.0 | 44.0 | 53.1 | 46.9 | 40.8 | 59.2 |

*Notes:* This table reports summary statistics of benefits in thousands of dollars and monthly benefit adjustments for four ages of interest (75, 85, 95, and 105 years old) and for the two allocation strategies. We consider the basic setting of Section 5 with the long-memory mortality model (see Section SM.H for additional details). The proportion value for the dynamic case reports the proportion of scenarios with a higher value of benefit (or benefit adjustment) for the dynamic strategy when compared to the static case. The proportion value for the static case is the opposite.

## Appendix. Supplementary material

Supplementary material related to this article can be found online at https://doi.org/10.1016/j.insmatheco.2024.05.006.

## References


Amaya, D., Bégin, J.-F., Gauthier, G., 2022. The informational content of high-frequency option prices. Manag. Sci. 68 (3), 2166–2201.

Andersen, T.G., Bollerslev, T., Diebold, F.X., 2007. Roughing it up: including jump components in the measurement, modeling, and forecasting of return volatility. Rev. Econ. Stat. 89 (4), 701–720.

Andrews, G.E., Askey, R., Roy, R., 1999. Special Functions. Encyclopedia of Mathematics and Its Applications. Cambridge University Press, Cambridge, UK.

Audrino, F., Knaus, S.D., 2016. Lassoing the HAR model: a model selection perspective on realized volatility dynamics. Econom. Rev. 35 (8–10), 1485–1521.

Babbs, S.H., Nowman, K.B., 1999. Kalman filtering of generalized Vasicek term structure models. J. Financ. Quant. Anal. 34 (1), 115–130.

Bakshi, G., Cao, C., Chen, Z., 1997. Empirical performance of alternative option pricing models. J. Finance 52 (5), 2003–2049.

Balter, A.G., Kallestrup-Lamb, M., Rangvid, J., 2020. Variability in pension products: a comparison study between the Netherlands and Denmark. Ann. Actuar. Sci. 14 (2), 338–357.

Balter, A.G., Werker, B.J., 2020. The effect of the assumed interest rate and smoothing on variable annuities. ASTIN Bull. 50 (1), 131–154.

Bandi, F.M., Renò, R., 2016. Price and volatility co-jumps. J. Financ. Econ. 119 (1), 107–146.

Bates, D.S., 1996. Jumps and stochastic volatility: exchange rate processes implicit in Deutsche mark options. Rev. Financ. Stud. 9 (1), 69–107.

Bates, D.S., 2000. Post-'87 crash fears in the S&P 500 futures option market. J. Econom. 94 (1–2), 181–238.

Bégin, J.-F., 2020. Levelling the playing field: a VIX-linked structure for funded pension schemes. Insur. Math. Econ. 94, 58–78.

Bégin, J.-F., Amaya, D., Gauthier, G., Malette, M.-E., 2020. On the estimation of jump-diffusion models using intraday data: a filtering-based approach. SIAM J. Financ. Math. 11 (4), 1168–1208.

Bégin, J.-F., Kapoor, N., Sanders, B., 2023a. A new approximation of annuity prices for age–period–cohort models. Eur. Actuar. J. https://doi.org/10.1007/s13385-023-00370-4.

Bégin, J.-F., Sanders, B., 2023. Benefit at risk in lifetime pension pools. Tech. Rep. Society of Actuaries and Canadian Institute of Actuaries, Ottawa, ON, Canada.

Bégin, J.-F., Sanders, B., Xu, X., 2023b. Modeling and forecasting subnational mortality in the presence of aggregated data. N. Am. Actuar. J. https://doi.org/10.1080/10920277.2023.2231996.

Bégin, J.-F., Sanders, B., Zhou, W., 2024. On the benefits of pension plan consolidation: understanding the impact of full plan mergers. Ann. Actuar. Sci. https://doi.org/10.1017/S1748499524000150.

Bernhardt, T., Donnelly, C., 2019. Modern tontine with bequest: innovation in pooled annuity products. Insur. Math. Econ. 86, 168–188.

Bernhardt, T., Donnelly, C., 2021. Quantifying the trade-off between income stability and the number of members in a pooled annuity fund. ASTIN Bull. 51 (1), 101–130.

Bollerslev, T., 1986. Generalized autoregressive conditional heteroskedasticity. J. Econom. 31 (3), 307–327.

Bongaerts, D., Kang, X., van Dijk, M., 2020. Conditional volatility targeting. Financ. Anal. J. 76 (4), 54–71.

Bowers, N.L.J., Gerber, H.U., Hickman, J.C., Jones, D.A., Nesbitt, C.J., 1997. Actuarial Mathematics. The Society of Actuaries, Schaumburg, IL, United States of America.

Boyle, P., Hardy, M., MacKay, A., Saunders, D., 2015. Variable payout annuities. Tech. Rep. Society of Actuaries, Schaumburg, IL, United States of America.

Brown, J.R., 2009. Understanding the role of annuities in retirement planning. In: Lusardi, A. (Ed.), Overcoming the Savings Slump: How to Increase the Effectiveness of Financial Education and Saving Programs. University of Chicago Press Chicago, Chicago, IL, United States of America, pp. 178–206. Chap. 6.

Busch, T., Christensen, B.J., Nielsen, M.Ø., 2011. The role of implied volatility in forecasting future realized volatility and jumps in foreign exchange, stock, and bond markets. J. Econom. 160 (1), 48–57.

Cairns, A.J., Blake, D., Dowd, K., 2006. A two-factor model for stochastic mortality with parameter uncertainty: theory and calibration. J. Risk Insur. 73 (4), 687–718.

Chen, A., Guillen, M., Rach, M., 2021. Fees in tontines. Insur. Math. Econ. 100, 89–106.

Chen, A., Rach, M., 2019. Options on tontines: an innovative way of combining tontines and annuities. Insur. Math. Econ. 89, 182–192.

Christoffersen, P., Heston, S., Jacobs, K., 2009. The shape and term structure of the index option smirk: why multifactor stochastic volatility models work so well. Manag. Sci. 55 (12), 1914–1932.
Cont, R., 2001. Empirical properties of asset returns: stylized facts and statistical issues. Quant. Finance 1 (2), 223.
Corsi, F., 2009. A simple approximate long-memory model of realized volatility. J. Financ. Econom. 7 (2), 174–196.
Corsi, F., Renò, R., 2012. Discrete-time volatility forecasting with persistent leverage effect and the link with continuous-time volatility modeling. J. Bus. Econ. Stat. 30 (3), 368–380.
Dees, B., de Jong, F., Nijman, T.E., 2021. Variable annuities with financial risk and longevity risk in the decumulation phase of Dutch DC products. Working Paper.
Di Maggio, M., Egan, M., Franzoni, F., 2022. The value of intermediation in the stock market. J. Financ. Econ. 145 (2), 208–233.
Doan, B., Papageorgiou, N., Reeves, J.J., Sherris, M., 2018. Portfolio management with targeted constant market volatility. Insur. Math. Econ. 83, 134–147.
Donnelly, C., 2015. Actuarial fairness and solidarity in pooled annuity funds. ASTIN Bull. 45 (1), 49–74.
Donnelly, C., Guillén, M., Nielsen, J.P., 2013. Exchanging uncertain mortality for a cost. Insur. Math. Econ. 52 (1), 65–76.
Donnelly, C., Guillén, M., Nielsen, J.P., 2014. Bringing cost transparency to the life annuity market. Insur. Math. Econ. 56, 14–27.
Dowd, K., Cairns, A.J., Blake, D., 2020. CBDX: a workhorse mortality model from the Cairns–Blake–Dowd family. Ann. Actuar. Sci. 14 (2), 445–460.
Duffie, D., Pan, J., Singleton, K., 2000. Transform analysis and asset pricing for affine jump-diffusions. Econometrica 68 (6), 1343–1376.
Engle, R.F., 1982. Autoregressive conditional heteroscedasticity with estimates of the variance of United Kingdom inflation. Econometrica 50 (4), 987–1007.
Eraker, B., 2004. Do stock prices and volatility jump? Reconciling evidence from spot and option prices. J. Finance 59 (3), 1367–1403.
Eraker, B., Johannes, M., Polson, N., 2003. The impact of jumps in volatility and returns. J. Finance 58 (3), 1269–1300.
Fleming, J., Kirby, C., Ostdiek, B., 2001. The economic value of volatility timing. J. Finance 56 (1), 329–352.
Fullmer, R.K., 2019. Tontines: a practitioner's guide to mortality-pooled investments. Tech. Rep. CFA Institute Research Foundation, Charlottesville, VA, United States of America.
Fung, M.C., Peters, G.W., Shevchenko, P.V., 2017. A unified approach to mortality modelling using state-space framework: characterisation, identification, estimation and forecasting. Ann. Actuar. Sci. 11 (2), 343–389.
Gemmo, I., Rogalla, R., Weinert, J.-H., 2020. Optimal portfolio choice with tontines under systematic longevity risk. Ann. Actuar. Sci. 14 (2), 302–315.
Girosi, F., King, G., 2008. Demographic Forecasting. Princeton University Press, Princeton, NJ, United States of America.
Gordon, N.J., Salmond, D.J., Smith, A.F., 1993. Novel approach to nonlinear/non-Gaussian Bayesian state estimation. IEE Proc., F, Radar Signal Process. 140 (2), 107–113.
Hallerbach, W.G., 2012. A proof of the optimality of volatility weighting over time. J. Invest. Strategy 1 (4), 87–99.
Hanewald, K., Piggott, J., Sherris, M., 2013. Individual post-retirement longevity risk management under systematic mortality risk. Insur. Math. Econ. 52 (1), 87–97.
Harvey, C.R., Hoyle, E., Korgaonkar, R., Rattray, S., Sargaison, M., Van Hemert, O., 2018. The impact of volatility targeting. J. Portf. Manag. 45 (1), 14–33.
Hocquard, A., Ng, S., Papageorgiou, N., 2013. A constant-volatility framework for managing tail risk. J. Portf. Manag. 39 (2), 28–40.
Horneff, W.J., Maurer, R.H., Mitchell, O.S., Stamos, M.Z., 2010. Variable payout annuities and dynamic portfolio choice in retirement. J. Pension Econ. Finance 9 (2), 163–183.
Iwry, J.M., Haldeman, C., Gale, W.G., John, D., 2020. Retirement tontines: Using a classical finance mechanism as an alternative source of retirement income. Working Paper.
Jacod, J., Todorov, V., 2009. Testing for common arrivals of jumps for discretely observed multidimensional processes. Ann. Stat. 37 (4), 1792–1838.
Johannes, M.S., Polson, N.G., Stroud, J.R., 2009. Optimal filtering of jump diffusions: extracting latent states from asset prices. Rev. Financ. Stud. 22 (7), 2759–2799.
Kalman, R.E., 1960. A new approach to linear filtering and predictive problems. J. Basic Eng. 82 (1), 35–45.
Lee, R.D., Carter, L.R., 1992. Modeling and forecasting US mortality. J. Am. Stat. Assoc. 87 (419), 659–671.
Li, S., Labit Hardy, H., Sherris, M., Villegas, A.M., 2022. A managed volatility investment strategy for pooled annuity products. Risks 10 (6), 121.
Litterman, R., Scheinkman, J., 1991. Common factors affecting bond returns. J. Fixed Income 1 (1), 54–61.
Liu, F., Tang, X., Zhou, G., 2019. Volatility-managed portfolio: does it really work? J. Portf. Manag. 46 (1), 38–51.
Milevsky, M.A., Salisbury, T.S., 2015. Optimal retirement income tontines. Insur. Math. Econ. 64, 91–105.
Milevsky, M.A., Salisbury, T.S., 2016. Equitable retirement income tontines: mixing cohorts without discriminating. ASTIN Bull. 46 (3), 571–604.
Moreira, A., Muir, T., 2017. Volatility-managed portfolios. J. Finance 72 (4), 1611–1644.
Mylnikov, G., 2021. Volatility targeting: it's complicated! J. Portf. Manag. 47 (8), 57–74.
Olivieri, A., Thirurajah, S., Ziveyi, J., 2022. Target volatility strategies for group self-annuity portfolios. ASTIN Bull. 52 (2), 591–617.
Pan, J., 2002. The jump-risk premia implicit in options: evidence from an integrated time-series study. J. Financ. Econ. 63 (1), 3–50.
Peters, G.W., Yan, H., Chan, J., 2021. Statistical features of persistence and long memory in mortality data. Ann. Actuar. Sci. 15 (2), 291–317.
Piggott, J., Valdez, E.A., Detzel, B., 2005. The simple analytics of a pooled annuity fund. J. Risk Insur. 72 (3), 497–520.
Plat, R., 2009. On stochastic mortality modeling. Insur. Math. Econ. 45 (3), 393–404.
Qiao, C., Sherris, M., 2013. Managing systematic mortality risk with group self-pooling and annuitization schemes. J. Risk Insur. 80 (4), 949–974.
Stamos, M.Z., 2008. Optimal consumption and portfolio choice for pooled annuity funds. Insur. Math. Econ. 43 (1), 56–68.
Todorov, V., Tauchen, G., 2011. Volatility jumps. J. Bus. Econ. Stat. 29 (3), 356–371.
Valdez, E.A., Piggott, J., Wang, L., 2006. Demand and adverse selection in a pooled annuity fund. Insur. Math. Econ. 39 (2), 251–266.
Vasicek, O., 1977. An equilibrium characterization of the term structure. J. Financ. Econ. 5 (2), 177–188.
Weinert, J.-H., Gründl, H., 2021. The modern tontine: an innovative instrument for longevity risk management in an aging society. Eur. Actuar. J. 11 (1), 49–86.
Zhang, L., Mykland, P.A., Aït-Sahalia, Y., 2005. A tale of two time scales: determining integrated volatility with noisy high-frequency data. J. Am. Stat. Assoc. 100 (472), 1394–1411.
Zhou, K.Q., Li, J.S.-H., 2023. The impact of long memory in mortality differentials on index-based longevity hedges. J. Demogr. Econ. 89 (3), 533–552.
Zhu, N., Bauer, D., 2022. Modeling the risk in mortality projections. Oper. Res. 70 (4), 2069–2084.